

Electronic Supplementary Information (ESI) for

Chiral coordination compounds with exceptional enantioselectivity

*Minju Lee and Kang Min Ok**

Department of Chemistry, Sogang University, 35 Baekbeom-ro, Mapo-gu, Seoul 04107, Republic of
Korea

Table of Contents

Sections	Titles	pages
Materials and Methods		S3-S4
Scheme S1	Synthesis of (<i>R,R</i>)-TBPG and (<i>S,S</i>)-TBPG	S3
Table S1	Crystallographic Data for (<i>R</i>)-Zn and (<i>S</i>)-Zn	S4
Fig. S1	¹ H and ¹³ C NMR spectra for (a) (<i>R,R</i>)-TBPG and (b) (<i>S,S</i>)-TBPG	S5-S6
Fig. S2	Ball-and-stick model revealing coordination modes of Zn ²⁺ cations and TBPG ligands in (<i>R</i>)-Zn	S7
Table S2	Selected bond distances (Å) and selected bond angles (°) for (<i>R</i>)-Zn	S8
Table S3	Hydrogen bonds distances (Å) for (<i>R</i>)-Zn	S9
Table S4	Selected bond distances (Å) and selected bond angles (°) for (<i>S</i>)-Zn	S10
Table S5	Hydrogen bonds distances (Å) for (<i>S</i>)-Zn	S11
Fig. S3	Experimental and calculated powder X-ray diffraction patterns of (<i>R</i>)-Zn and (<i>S</i>)-Zn	S12
Fig. S4	EDX data for (<i>R</i>)-Zn and (<i>S</i>)-Zn	S13
Fig. S5	IR spectra for (<i>R,R</i>)-TBPG, (<i>S,S</i>)-TBPG, (<i>R</i>)-Zn and (<i>S</i>)-Zn	S14
Fig. S6	UV-vis diffuse reflectance spectra for (<i>R,R</i>)-TBPG, (<i>S,S</i>)-TBPG, (<i>R</i>)-Zn and (<i>S</i>)-Zn	S15
Fig. S7	TGA diagrams for (<i>R</i>)-Zn and (<i>S</i>)-Zn	S16
Fig. S8	PXRD patterns measured after heating the title compounds to 800 °C	S16
Fig. S9	(a) Solid-state CD spectra of (<i>R,R</i>)-TBPG, (<i>S,S</i>)-TBPG, (<i>R</i>)-Zn, and (<i>S</i>)-Zn. (b) Absorbance spectra of (<i>R,R</i>)-TBPG and (<i>R</i>)-Zn	S17
Fig. S10	Band structures for (a) (<i>R</i>)-Zn and (b) (<i>S</i>)-Zn	S18
Fig. S11	Total and partial density of states for (a) (<i>R</i>)-Zn and (b) (<i>S</i>)-Zn	S18
Fig. S12	Plots of SHG intensity versus particle size for (<i>R</i>)-Zn and (<i>S</i>)-Zn	S19
Table S6	Dipole moments for polyhedra in (<i>R</i>)-Zn and (<i>S</i>)-Zn	S20
Fig. S13	Net moments and dipole moments of ZnO ₆ polyhedra in a unit cell	S20
Fig. S14	PXRD patterns revealing the stability of (<i>R</i>)-Zn (a) in various solvents and (b) at various pH values.	S21
Table S7	Crystallographic Data for (<i>S</i>)-Zn-EtOH	S22
Table S8	Selected bond distances (Å) and selected bond angles (°) for (<i>S</i>)-Zn-EtOH	S23
Table S9	Hydrogen bonds distances (Å) for (<i>S</i>)-Zn-EtOH	S24
Fig. S15	Experimental and calculated powder X-ray diffraction patterns of (<i>S</i>)-Zn-EtOH	S25
Fig. S16	GC-MS results of distilled ethyl ether	S26-S27
Fig. S17	GC-MS result of distilled ethyl ether containing (<i>S</i>)-Zn crystal for 1 day	S28-S29
Fig. S18	GC-MS results of distilled ethyl ether containing (<i>S</i>)-Zn for crystal 3 days	S30-S31
Fig. S19	GC-MS results of distilled ethyl ether containing (<i>S</i>)-Zn for crystal 7 days	S32-S33
Fig. S20	GC-MS results of distilled ethyl ether containing (<i>S</i>)-Zn for crystal 10 days	S34-S35
Fig. S21	GC-MS results of distilled ethyl ether containing (<i>S</i>)-Zn for crystal 14 days	S36-S37
Fig. S22	GC-MS results of distilled ethyl ether containing Zn(NO ₃) ₂ for 1 day	S38-S39
Fig. S23	GC-MS results of distilled ethyl ether containing TBPG ligand for 1 day	S40-S41
Fig. S24	Fluorescence emission spectra of (<i>R</i>)-Zn and (<i>R,R</i>)-TBPG in the solid state	S42
Fig. S25	PXRD patterns of (<i>R</i>)-Zn before and after the fluorescence measurements	S43
Fig. S26	Fluorescence emission spectra of (<i>R,R</i>)-TBPG upon addition of (a) D- and (b) L-Histidine	S44
Fig. S27	Stern-Volmer (SV) plots of (<i>R,R</i>)-TBPG + D-Histidine and (<i>R,R</i>)-TBPG + L-Histidine.	S44
Fig. S28	Fluorescence emission spectra of (<i>R</i>)-Zn upon addition of imidazole	S45
Fig. S29	Stern-Volmer (SV) plots of (<i>R</i>)-Zn + D-Histidine, (<i>R</i>)-Zn + L-Histidine and (<i>R</i>)-Zn + imidazole	S45
Fig. S30	¹ H NMR spectra for (<i>R</i>)-Zn in DMSO-d ₆ , (<i>R</i>)-Zn + Histidine in DMSO-d ₆ /D ₂ O and Histidine in D ₂ O	S46
Fig. S31	Fluorescence emission spectra of (<i>S</i>)-Zn upon addition of (a) D- and (b) L-Histidine	S47
Fig. S32	Stern-Volmer (SV) plots of (<i>S</i>)-Zn + D-Histidine, (<i>R</i>)-Zn + L-Histidine	S47

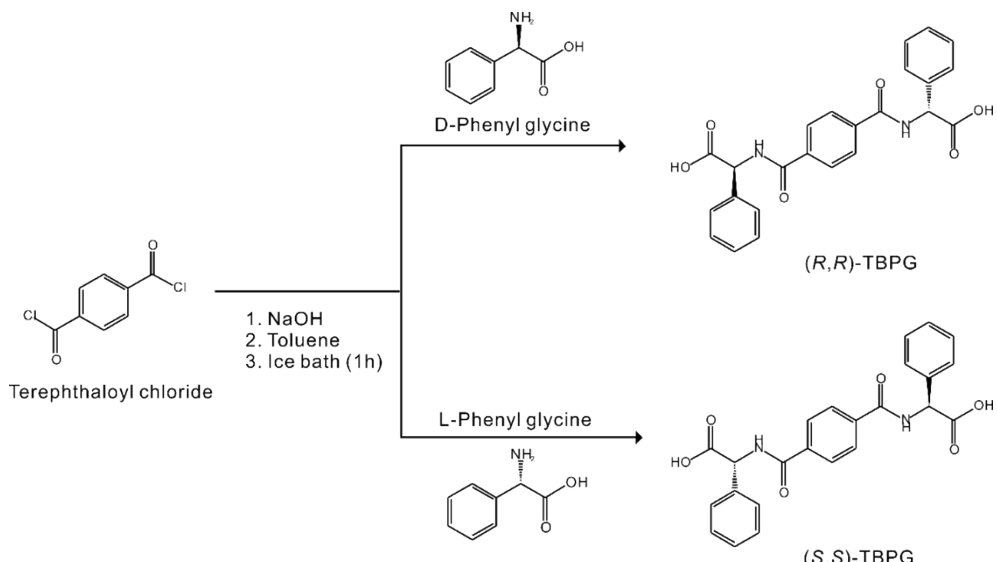
Experimental Procedures

Section S1. Materials and Methods

Materials. D-2-phenylglycine (99%, TCI), L-2-phenylglycine (98%, TCI), $Zn(NO_3)_2 \cdot 6H_2O$ (99%, Alfa Aesar), NaOH (98%, Alfa Aesar), Terephthaloyl chloride (99%, Sigma Aldrich), Toluene (99.8%, Samchun), HCl (35~37 wt% aq. solution, Samchun), *N,N'*-dimethylacetamide (DMA, 99%, Alfa Aesar), ethanol (99.9%, Samchun), and dimethyl sulfoxide-d₆ (99%, Sigma Aldrich) were purchased and used without further purification.

Synthesis of (*R,R*)-Terephthaloyl-bis-phenyl glycine [(*R,R*)-TBPG] and (*S,S*)-Terephthaloyl-bis-phenyl glycine [(*S,S*)-TBPG] ligands. The (*R,R*)-TBPG ligand was synthesized by a nucleophilic aromatic substitution reaction (Scheme S1). A 1.5 g (10.0 mmol) portion of D-phenyl glycine and 0.6 g (15.0 mmol) of NaOH were placed in a round bottom flask and dissolved in 20 mL of water by stirring in an ice bath to cool the solution to below 10 °C. And then, 1.0 g (5.0 mmol) of terephthaloyl chloride dissolved in 20 mL of toluene solution was added dropwise to the mixture. After the reaction mixture was stirred for 1 h, the aqueous layer was separated from the organic layer and acidified with concentrated HCl aqueous solution. The white product was collected by a vacuum filtration and dried. (*S,S*)-TBPG was synthesized by the same method as that of (*R,R*)-TBPG using L-phenyl glycine instead of D-phenyl glycine. (*R,R*)-TBPG and (*S,S*)-TBPG were obtained in 92.0% and 93.5% yields, respectively.

Scheme S1. Synthesis of (*R,R*)-TBPG and (*S,S*)-TBPG



Synthesis of $[Zn_2((R,R\text{-})\text{TBPG})_2(H_2O)_5]\cdot 4H_2O$ [(*R*)-Zn] and $[Zn_2((S,S\text{-})\text{TBPG})_2(H_2O)_5]\cdot 4H_2O$ [(*S*)-Zn]. A 0.089 g (0.3 mmol) portion of $Zn(NO_3)_2 \cdot 6H_2O$, 0.130 g (0.3 mmol) of (*R,R*)-TBPG or (*S,S*)-TBPG, 1 mL of DMA, 1 mL of deionized water, and 1 mL of ethanol were put into a Teflon-lined autoclave. After closing, the autoclave was heated at 80 °C for 72 h and cooled to room temperature at a rate of 6 °C/h. The clear solution was transferred to a vial and colorless plate-shaped crystals begin to grow after about 5 hours through slow evaporation. After 24 h, the complete product was filtered and washed with deionized water. Colorless crystals of (*R*)-Zn and (*S*)-Zn were obtained in 43% and 41% yields, respectively.

Instrumentation. Colorless plate shape single crystals with the size of 0.168 mm × 0.153 mm × 0.037 mm for (*R*)-Zn and 0.164 mm × 0.157 mm × 0.104 mm for (*S*)-Zn were used for single crystal X-ray diffraction (SC-XRD) analysis. SC-XRD data were collected using a Bruker D8 QUEST diffractometer with a graphite monochromated Mo Kα radiation source ($\lambda = 0.71703 \text{ \AA}$) and a PHOTON-II CPAD detector at 100 K at the Advanced Bio-Interface Core Research Facility, Sogang University. The collected data were integrated by the SAINT program¹ and absorption correction was performed using the program SADABS.^{2,3} The crystal structures were solved and refined with SHELXS-2013 and SHELXL-2013, respectively, implemented in the WinGX-2014.⁴⁻⁶ Since the solvent molecules were severely disordered, the SQUEEZE option in the PLATON^{7,8} software was performed. The detailed crystallographic data for (*R*)-Zn and (*S*)-Zn are tabulated in Table S1. The diffraction data for (*S*)-Zn-EtOH were obtained using a synchrotron radiation (0.63000 Å) on the 2D Supramolecular Crystallography (2D-SMC) beamline equipped with a Rayonix MX225HS CCD area detector at 100k in Pohang Acceleration Laboratory (PAL). The data were integrated and scaled by the program HKL-3000sm.⁹ The crystal structures were solved and refined with SHELXS-2013⁴ and SHELXL-2013,⁵ respectively, implemented in the WinGX-2014.⁶ Since the solvent molecules were severely disordered, the SQUEEZE option in the PLATON^{7,8} software was performed. The detailed crystallographic data and selected bond lengths and selected bond angles for (*S*)-Zn-EtOH are tabulated in Tables S7-9.

Table 1 Crystallographic Data for (*R*)-Zn and (*S*)-Zn

	(<i>R</i>)-Zn	(<i>S</i>)-Zn
fw	1153.69	1153.69
space group	<i>P</i> 2 ₁	<i>P</i> 2 ₁
<i>a</i> (Å)	12.0803(13)	12.0909(7)
<i>b</i> (Å)	16.6380(18)	16.6580(10)
<i>c</i> (Å)	14.6323(16)	14.6039(8)
β (°)	114.205(4)	114.138(2)
<i>V</i> (Å ³)	2682.45(5)	2684.2(3)
<i>Z</i>	2	2
<i>T</i> (K)	100(2)	100(2)
λ (Å)	0.71073	0.71073
ρ_{calcd} (g/cm ³)	1.428	1.410
<i>R</i> (<i>F</i> _o) ^a	0.0664	0.0461
<i>R</i> _w (<i>F</i> _o ²) ^b	0.1047	0.0601
Flack <i>x</i>	0.042(6)	0.042(4)

$$^aR(F) = \sum | |F_o| - |F_c| | / \sum |F_o|. \quad ^bR_w(F_o^2) = [\sum w(F_o^2 - F_c^2)^2 / \sum w(F_o^2)^2]^{1/2}.$$

Powder X-ray diffraction (PXRD) data were collected on a Rigaku MiniFlex 600 using Cu K α ($\lambda = 1.5406$ Å) radiation with 40 kV and 15 mA at room temperature. Polycrystalline samples were placed on the sample holders and then scanned in the 2 θ range of 5–70° with a scan speed of 20° min⁻¹ and a scan step width of 0.02°.

Thermogravimetric analysis (TGA) diagrams of the title compounds were obtained by using a SCINCO TGA-N1000 thermal analyzer. The polycrystalline samples were placed on alumina crucibles and heated from 25 °C to 900 °C at a rate of 10 °C min⁻¹ under flowing air.

¹H-NMR and ¹³C-NMR spectral data of the samples were measured with a Varian Inova 400 spectrometer at 400 and 100 MHz, respectively.

Energy Dispersive X-ray Spectrometer (EDX) data were measured with a Horiba Energy EX-250 instrument equipped on a Hitachi S-3400N scanning electron microscope. The EDX data matched well with the calculated atomic ratios obtained from SC-XRD.

Elemental analysis was measured with a Thermo Scientific Flash 2000 on Sn capsules. Elemental analysis for (*R*)-Zn, observed (calculated): C, 49.97% (49.88%); H, 4.72% (4.74%); N, 4.84% (4.91%); (*S*)-Zn, observed (calculated): C, 49.91% (49.88%); H, 4.84 (4.74%); N, 4.82% (4.91%).

Infrared (IR) spectra were measured with a Thermo Scientific Nicolet iS50 FT-IR spectrometer in the range of 400–4000 cm⁻¹ with an attenuated total reflection (ATR) accessory.

UV-vis diffuse-reflectance spectra were measured with a Jasco V-660 spectrophotometer in the range of 200–800 nm. The band gap energy was calculated by the Kubelka-Munk function.¹⁰

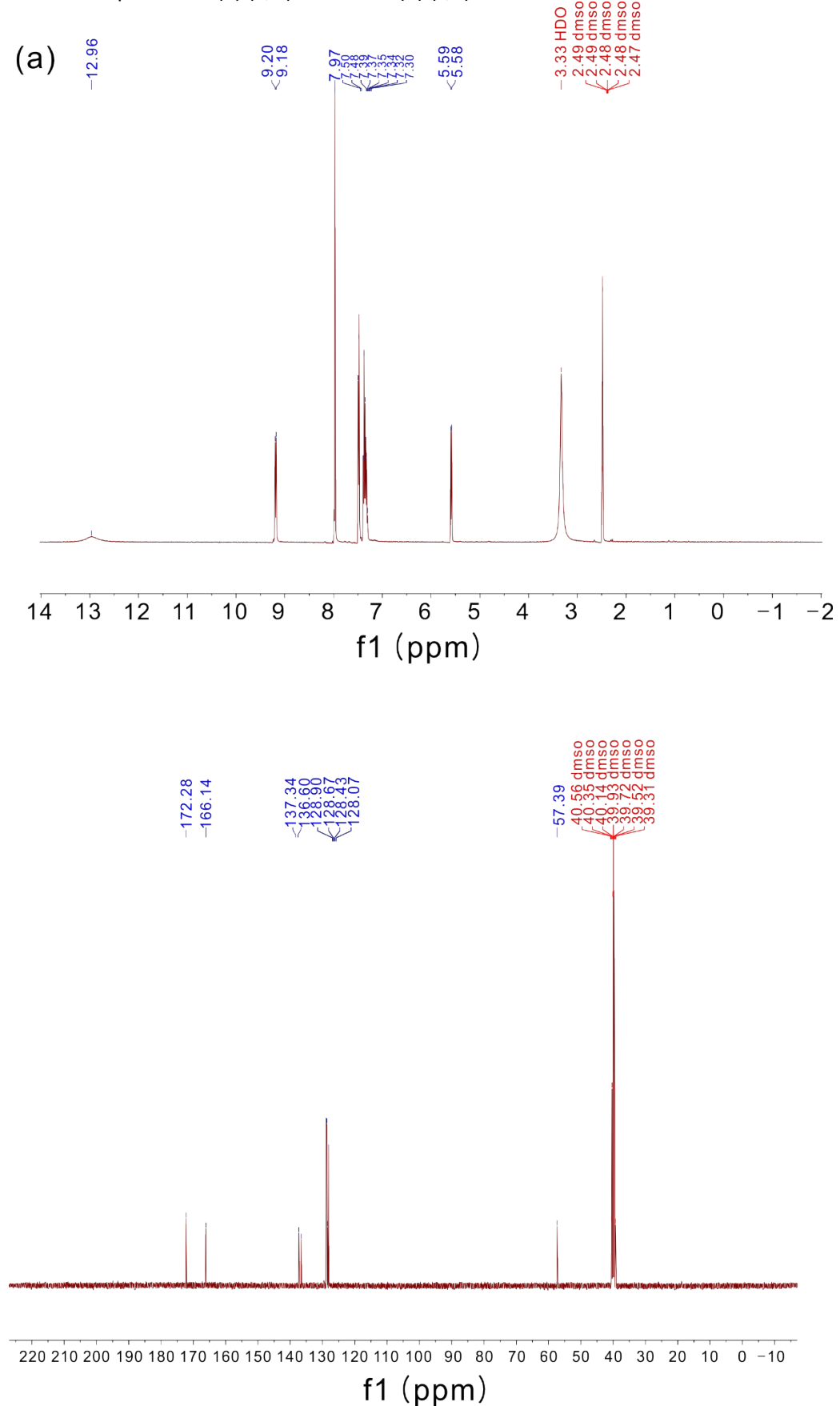
Density functional theory (DFT) calculations for title compounds were performed to investigate the electronic structures using the Quantum Espresso package.¹¹ The ultrasoft pseudopotentials type¹² and the Perdew–Burke–Ernzerhof (PBE)¹³ functionals were used for all elements (C, H, N, O, and Zn). The kinetic energy and charge density cutoff were set to 46.649 and 419.846 Ry, respectively. The self-consistent function (SCF) convergence thresholds were set to about 4.0×10^{-6} Ry and the k-points grids of Brillouin zone was set to $2 \times 2 \times 2$.

Solid state circular dichroism (CD) spectra were measured with a JASCO-J-815 spectrophotometer in the range of 220–325 nm after purging with nitrogen gas. The scanning speeds for the measurements were 50 nm min⁻¹.

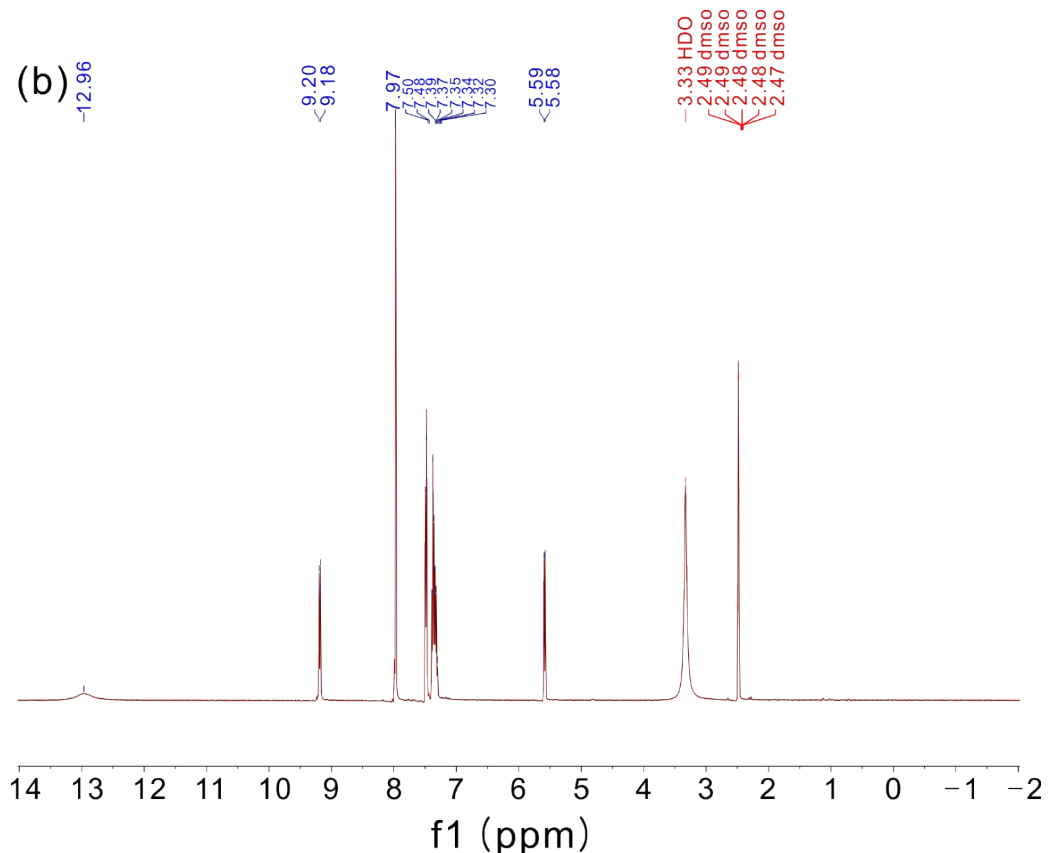
The fluorescence spectra were measured with a Hitachi F-7000 fluorescence spectrophotometer in the range of 600–800 nm. The scanning speeds for the measurements were 1200 nm min⁻¹. The solid-state fluorescence measurements for (*R*)-Zn were performed at room temperature. To investigate the selective sensing capacity of (*R*)-Zn for Histidine, the ground polycrystalline sample of (*R*)-Zn (10 mg) was dispersed in water (3 mL) by ultrasonication and then subsequently placed in a cuvette with 1 cm width for the measurements. All the titrations were carried out by adding L- and D-Histidine (10 mM) gradually. The fluorescence spectra were recorded at 298 K with the emission wavelength at 680 nm ($\lambda_{\text{ex}} = 340$ nm). Each measurement was repeated three times to obtain reliable data.

Powder second-harmonic generation (SHG) measurements were performed using a modified Kurtz nonlinear optical system.¹⁴ Because the SHG efficiency depends on the particle size, the ground sample was sieved into specific particle size ranges (< 20, 20–45, 45–63, 63–75, 75–90, and 90–125 μm). Each sieved particle was put into separate capillary tubes. The tubes were irradiated by a DAWA Q-switched Nd:YAG laser (1064 nm), and the SHG light (532 nm) was received to a Hamamatsu photomultiplier tube and detected by a Tektronix TDS 1032 oscilloscope. A comprehensive SHG measurement was described earlier in the published paper.¹⁵

Fig. S1 ^1H and ^{13}C NMR spectra for (a) (*R,R*)-TBPG and (b) (*S,S*)-TBPG



(b)



(c)

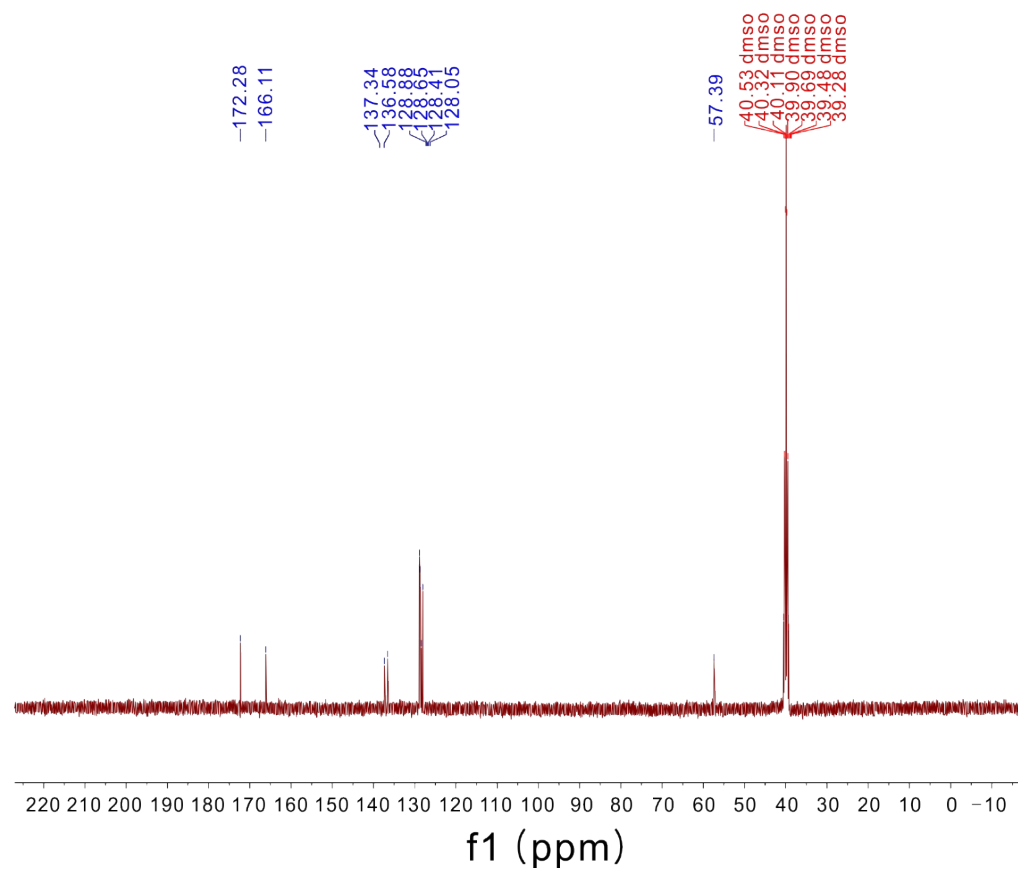


Fig. S2 Ball-and-stick model revealing coordination modes of Zn^{2+} cations and TBPB ligands in (*R*)-Zn (cyan, Zn; black, C; red, O).

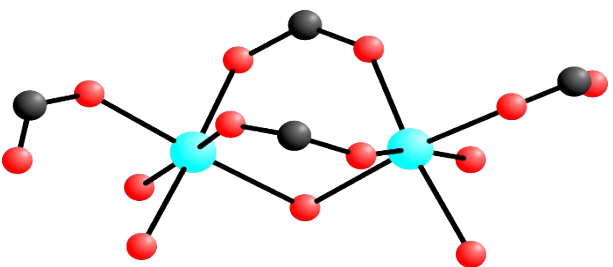


Table S2 Selected bond distances (\AA) and selected bond angles ($^\circ$) for (R)-Zn

Selected bond distances (\AA)							
Zn(1)-O(4)	2.031(5)	Zn(2)-O(11)	2.287(6)	O(16)-C(48)	1.252(9)	C(37)-C(40)	1.494(10)
Zn(1)-O(17)#1	2.074(5)	O(4)-C(1)	1.252(8)	O(17)-C(48)	1.259(8)	C(41)-C(42)	1.42(5)
Zn(1)-O(13)#2	2.086(5)	O(5)-C(1)	1.257(9)	C(1)-C(2)	1.531(10)	C(41)-C(48)	1.548(10)
Zn(1)-O(1)	2.096(6)	O(6)-C(9)	1.244(9)	C(2)-C(3)	1.503(11)	N(1)-C(9)	1.319(9)
Zn(1)-O(3)	2.136(5)	O(7)-C(16)	1.244(8)	C(9)-C(10)	1.496(10)	N(1)-C(2)	1.474(9)
Zn(1)-O(2)#2	2.163(6)	O(8)-C(24)	1.258(9)	C(13)-C(16)	1.500(10)	N(2)-C(16)	1.323(9)
Zn(2)-O(12)	2.027(5)	O(9)-C(24)	1.267(9)	C(17)-C(18)	1.525(10)	N(2)-C(17)	1.468(9)
Zn(2)-O(16)#3	2.042(5)	O(12)-C(25)	1.267(8)	C(17)-C(24)	1.522(10)	N(3)-C(33)	1.341(9)
Zn(2)-O(9)	2.056(5)	O(13)-C(25)	1.248(9)	C(25)-C(26)	1.518(10)	N(3)-C(26)	1.455(9)
Zn(2)-O(10)	2.072(5)	O(14)-C(33)	1.232(9)	C(26)-C(27)	1.523(10)	N(4)-C(40)	1.341(9)
Zn(2)-O(2)	2.186(5)	O(15)-C(40)	1.231(10)	C(33)-C(34)	1.502(10)	N(4)-C(41)	1.464(9)
Selected bond angles ($^\circ$)							
O(1)-Zn(1)-O(2)#2	90.3(2)	O(16)#3-Zn(2)-O(10)	92.0(2)	C(40)-N(4)-C(41)	122.4(7)		
O(1)-Zn(1)-O(3)	85.1(2)	O(16)#3-Zn(2)-O(11)	174.5(2)	O(4)-C(1)-C(2)	116.1(6)		
O(2)-Zn(2)-O(11)	89.6(2)	O(17)#1-Zn(1)-O(1)	92.9(2)	O(5)-C(1)-C(2)	116.7(6)		
O(3)-Zn(1)-O(2)#2	92.7(2)	O(17)#1-Zn(1)-O(2)#2	89.3(2)	O(6)-C(9)-C(10)	119.5(7)		
O(4)-Zn(1)-O(1)	85.7(2)	O(17)#1-Zn(1)-O(3)	177.2(2)	O(7)-C(16)-C(13)	119.2(6)		
O(4)-Zn(1)-O(2)#2	173.1(2)	O(17)#1-Zn(1)-O(13)#2	95.8(2)	O(8)-C(24)-C(17)	117.5(7)		
O(4)-Zn(1)-O(3)	92.7(20)	Zn(1)#4-O(2)-Zn(2)	111.4(2)	O(9)-C(24)-C(17)	116.7(6)		
O(4)-Zn(1)-O(13)#2	90.29(19)	C(1)-O(4)-Zn(1)	130.6(5)	O(12)-C(25)-C(26)	115.5(6)		
O(4)-Zn(1)-O(17)#1	85.2(2)	C(24)-O(9)-Zn(2)	128.4(5)	O(13)-C(25)-C(26)	117.0(6)		
O(9)-Zn(2)-O(2)	171.6(2)	C(25)-O(12)-Zn(2)	131.3(5)	O(14)-C(33)-C(34)	121.7(6)		
O(9)-Zn(2)-O(10)	92.4(2)	C(25)-O(13)-Zn(1)#4	132.7(5)	O(15)-C(40)-C(37)	121.3(7)		
O(9)-Zn(2)-O(11)	83.1(2)	C(48)-O(16)-Zn(2)#5	134.5(5)	O(16)-C(48)-C(41)	117.1(6)		
O(10)-Zn(2)-O(2)	91.0(2)	C(48)-O(17)-Zn(1)#6	132.0(5)	N(1)-C(2)-C(1)	110.2(6)		
O(10)-Zn(2)-O(11)	84.9(2)	O(4)-C(1)-O(5)	127.0(7)	N(1)-C(2)-C(3)	114.2(6)		
O(12)-Zn(2)-O(2)	87.9(2)	O(8)-C(24)-O(9)	125.8(7)	N(1)-C(9)-C(10)	117.7(6)		
O(12)-Zn(2)-O(11)	83.9(2)	O(13)-C(25)-O(12)	127.5(7)	N(2)-C(16)-C(13)	119.1(6)		
O(12)-Zn(2)-O(9)	87.2(2)	O(16)-C(48)-O(17)	127.2(7)	N(2)-C(17)-C(18)	112.7(6)		
O(12)-Zn(2)-O(10)	168.7(2)	O(6)-C(9)-N(1)	122.7(7)	N(2)-C(17)-C(24)	109.7(6)		
O(12)-Zn(2)-O(16)#3	99.3(2)	O(7)-C(16)-N(2)	121.7(7)	N(3)-C(26)-C(25)	110.7(6)		
O(13)#2-Zn(1)-O(1)	170.1(2)	O(14)-C(33)-N(3)	121.4(7)	N(3)-C(26)-C(27)	112.6(6)		
O(13)#2-Zn(1)-O(2)#2	94.4(2)	O(15)-C(40)-N(4)	121.3(7)	N(3)-C(33)-C(34)	116.9(6)		
O(13)#2-Zn(1)-O(3)	86.0(2)	C(9)-N(1)-C(2)	122.2(6)	N(4)-C(40)-C(37)	117.4(7)		
O(16)#3-Zn(2)-O(2)	94.9(2)	C(16)-N(2)-C(17)	119.7(6)	N(4)-C(41)-C(42)	110.6(13)		
O(16)#3-Zn(2)-O(9)	92.6(2)	C(33)-N(3)-C(26)	120.4(6)	N(4)-C(41)-C(48)	107.3(6)		
Symmetry operation : #1 x-1,y+1,z-1 #2 x,y+1,z #3 x-1,y,z-1 #4 x,y-1,z #5 x+1,y,z+1 #6 x+1,y-1,z+1							

Table S3 Hydrogen bonds distances (\AA) for (*R*)-Zn

D-H...A	d(D...A)	D-H...A	d(D...A)
N(1)-H(1)...O(18)#1	2.968(8)	O(10)-H(55)...O(7)#9	2.732(7)
N(2)-H(2A)...O(19)	3.477(9)	O(11)-H(56)...O(19)	2.812(9)
O(1)-H(48)...O(14)#7	2.734(7)	O(18)-H(58)...O(8)#8	2.868(8)
O(2)-H(50)...O(20)	2.600(8)	O(18)-H(59)...O(17)	2.825(7)
O(2)-H(51)...O(21)	2.634(8)	O(19)-H(60)...O(12)	2.762(8)
O(3)-H(52)...O(4)	3.016(7)	O(19)-H(61)...O(5) #8	2.840 (8)
O(3)-H(52)...O(5)	2.738(7)	O(20)-H(62)...O(6)#8	2.728(8)
O(3)-H(53)...O(6)#7	2.796(8)	O(20)-H(63)...O(11)	2.756(9)
O(10)-H(54)...O(8)	2.638(8)	O(21)-H(64)...O(7)#9	2.804(9)

Symmetry operation : #1 x-1,y+1,z-1 #7 -x+1,y+1/2,-z+1 #8 -x+1,y-1/2,-z+1 #9 -x,y-1/2,-z

Table S4 Selected bond distances (\AA) and selected bond angles ($^\circ$) for (S)-Zn

Selected bond distances (\AA)							
Zn(1)-O(4)	2.042(3)	Zn(2)-O(11)	2.284(4)	O(16)-C(48)	1.257(6)	C(37)-C(40)	1.501(7)
Zn(1)-O(17)#1	2.071(3)	O(4)-C(1)	1.252(6)	O(17)-C(48)	1.255(6)	C(41)-C(42)	1.47(4)
Zn(1)-O(13)#2	2.079(3)	O(5)-C(1)	1.248(6)	C(1)-C(2)	1.533(6)	C(41)-C(48)	1.540(7)
Zn(1)-O(1)	2.102(4)	O(6)-C(9)	1.252(5)	C(2)-C(3)	1.520(7)	N(1)-C(9)	1.318(6)
Zn(1)-O(3)	2.144(3)	O(7)-C(16)	1.242(6)	C(9)-C(10)	1.503(6)	N(1)-C(2)	1.475(6)
Zn(1)-O(2)	2.160(3)	O(8)-C(24)	1.250(5)	C(13)-C(16)	1.500(6)	N(2)-C(16)	1.336(6)
Zn(2)-O(12)	2.023(3)	O(9)-C(24)	1.270(5)	C(17)-C(18)	1.520(7)	N(2)-C(17)	1.465(6)
Zn(2)-O(16)#3	2.039(4)	O(12)-C(25)	1.259(5)	C(17)-C(24)	1.527(7)	N(3)-C(33)	1.343(6)
Zn(2)-O(9)	2.050(3)	O(13)-C(25)	1.245(6)	C(25)-C(26)	1.539(6)	N(3)-C(26)	1.461(5)
Zn(2)-O(10)	2.067(3)	O(14)-C(33)	1.222(6)	C(26)-C(27)	1.511(7)	N(4)-C(40)	1.342(6)
Zn(2)-O(2)#4	2.188(3)	O(15)-C(40)	1.225(6)	C(33)-C(34)	1.502(6)	N(4)-C(41)	1.461(6)
Selected bond angles ($^\circ$)							
O(1)-Zn(1)-O(2)	90.23(14)	O(16)#3-Zn(2)-O(10)	91.90(14)	C(40)-N(4)-C(41)	121.3(4)		
O(1)-Zn(1)-O(3)	85.13(14)	O(16)#3-Zn(2)-O(11)	174.54(14)	O(4)-C(1)-C(2)	115.6(4)		
O(2)#4-Zn(2)-O(11)	89.85(13)	O(17)#1-Zn(1)-O(1)	93.01(14)	O(5)-C(1)-C(2)	117.0(4)		
O(3)-Zn(1)-O(2)	92.87(13)	O(17)#1-Zn(1)-O(2)	88.89(13)	O(6)-C(9)-C(10)	119.0(4)		
O(4)-Zn(1)-O(1)	85.69(14)	O(17)#1-Zn(1)-O(3)	177.44(13)	O(7)-C(16)-C(13)	120.1(4)		
O(4)-Zn(1)-O(2)	172.90(13)	O(17)#1-Zn(1)-O(13)#2	95.56(14)	O(8)-C(24)-C(17)	117.7(4)		
O(4)-Zn(1)-O(3)	92.57(13)	Zn(1)-O(2)-Zn(2)#2	111.44(15)	O(9)-C(24)-C(17)	116.1(4)		
O(4)-Zn(1)-O(13)#2	90.43(12)	C(1)-O(4)-Zn(1)	130.2(3)	O(12)-C(25)-C(26)	115.0(4)		
O(4)-Zn(1)-O(17)#1	85.53(13)	C(24)-O(9)-Zn(2)	128.4(3)	O(13)-C(25)-C(26)	117.5(4)		
O(9)-Zn(2)-O(2)#4	172.02(13)	C(25)-O(12)-Zn(2)	131.7(3)	O(14)-C(33)-C(34)	121.7(4)		
O(9)-Zn(2)-O(10)	92.10(13)	C(25)-O(13)-Zn(1)#4	132.7(3)	O(15)-C(40)-C(37)	121.2(4)		
O(9)-Zn(2)-O(11)	83.18(13)	C(48)-O(16)-Zn(2)#5	134.5(3)	O(16)-C(48)-C(41)	117.1(4)		
O(10)-Zn(2)-O(2)#4	91.17(13)	C(48)-O(17)-Zn(1)#6	132.5(3)	N(1)-C(2)-C(3)	113.6(4)		
O(10)-Zn(2)-O(11)	85.03(14)	O(5)-C(1)-O(4)	127.4(4)	N(1)-C(2)-C(1)	110.6(4)		
O(12)-Zn(2)-O(2)#4	87.90(13)	O(8)-C(24)-O(9)	126.2(4)	N(1)-C(9)-C(10)	117.6(4)		
O(12)-Zn(2)-O(9)	87.52(13)	O(13)-C(25)-O(12)	127.4(4)	N(2)-C(16)-C(13)	119.3(4)		
O(12)-Zn(2)-O(10)	169.13(14)	O(17)-C(48)-O(16)	126.7(5)	N(2)-C(17)-C(18)	113.1(4)		
O(12)-Zn(2)-O(11)	84.14(13)	O(6)-C(9)-N(1)	123.4(4)	N(2)-C(17)-C(24)	110.1(4)		
O(12)-Zn(2)-O(16)#3	98.97(14)	O(7)-C(16)-N(2)	120.6(4)	N(3)-C(26)-C(27)	112.8(4)		
O(13)#2-Zn(1)-O(1)	170.29(14)	O(14)-C(33)-N(3)	121.6(4)	N(3)-C(26)-C(25)	109.6(4)		
O(13)#2-Zn(1)-O(2)	94.49(13)	O(15)-C(40)-N(4)	122.3(4)	N(3)-C(33)-C(34)	116.7(4)		
O(13)#2-Zn(1)-O(3)	86.16(14)	C(9)-N(1)-C(2)	121.1(4)	N(4)-C(40)-C(37)	116.5(5)		
O(16)#3-Zn(2)-O(2)#4	94.73(14)	C(16)-N(2)-C(17)	120.0(4)	N(4)-C(41)-C(42)	111.8(1)		
O(16)#3-Zn(2)-O(9)	92.44(14)	C(33)-N(3)-C(26)	119.7(4)	N(4)-C(41)-C(48)	107.5(4)		

Symmetry operation : #1 x-1,y-1,z-1 #2 x,y-1,z #3 x-1,y,z-1 #4 x,y+1,z #5 x+1,y,z+1 #6 x+1,y+1,z+1

Table S5 Hydrogen bonds distances (\AA) for (S)-Zn

D-H...A	d(D...A)	D-H...A	d(D...A)
N(1)-H(1)...O(18)#1	2.967(5)	O(10)-H(55)...O(8)	2.626(5)
N(2)-H(2A)...O(19)	3.468(6)	O(11)-H(57)...O(19)	2.814(5)
O(1)-H(48)...O(14)#10	2.743(5)	O(18)-H(58)...O(17)	2.833(5)
O(2)-H(50)...O(20)	2.640(5)	O(18)-H(59)...O(8)#8	2.862(5)
O(2)-H(51)...O(21)	2.613(5)	O(19)-H(60)...O(5)#8	2.843(5)
O(3)-H(52)...O(6)#10	2.799(5)	O(19)-H(61)...O(12)	2.773(5)
O(3)-H(53)...O(4)	3.027(5)	O(20)-H(63)...O(7)#9	2.808(5)
O(3)-H(53)...O(5)	2.744(5)	O(21)-H(64)...O(6)#10	2.716(5)
O(10)-H(54)...O(7)#7	2.743(5)	O(21)-H(65)...O(11)#2	2.749(6)

Symmetry operation : #1 x-1,y-1,z-1 #2 x,y-1,z #7 -x,y+1/2,-z #8 -x+1,y+1/2,-z+1 #9 -x,y-1/2,-z #10 -x+1,y-1/2,-z+1

Fig. S3 Experimental and calculated powder X-ray diffraction patterns of (*R*)-Zn and (*S*)-Zn

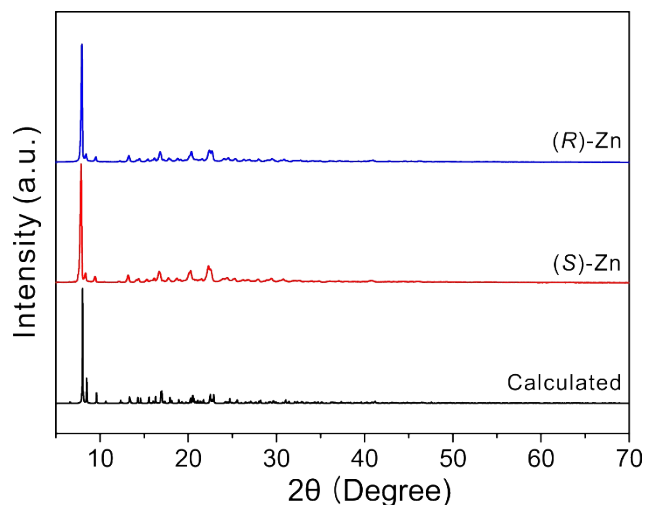


Fig. S4 SEM-EDX data for *(R)*-Zn and *(S)*-Zn

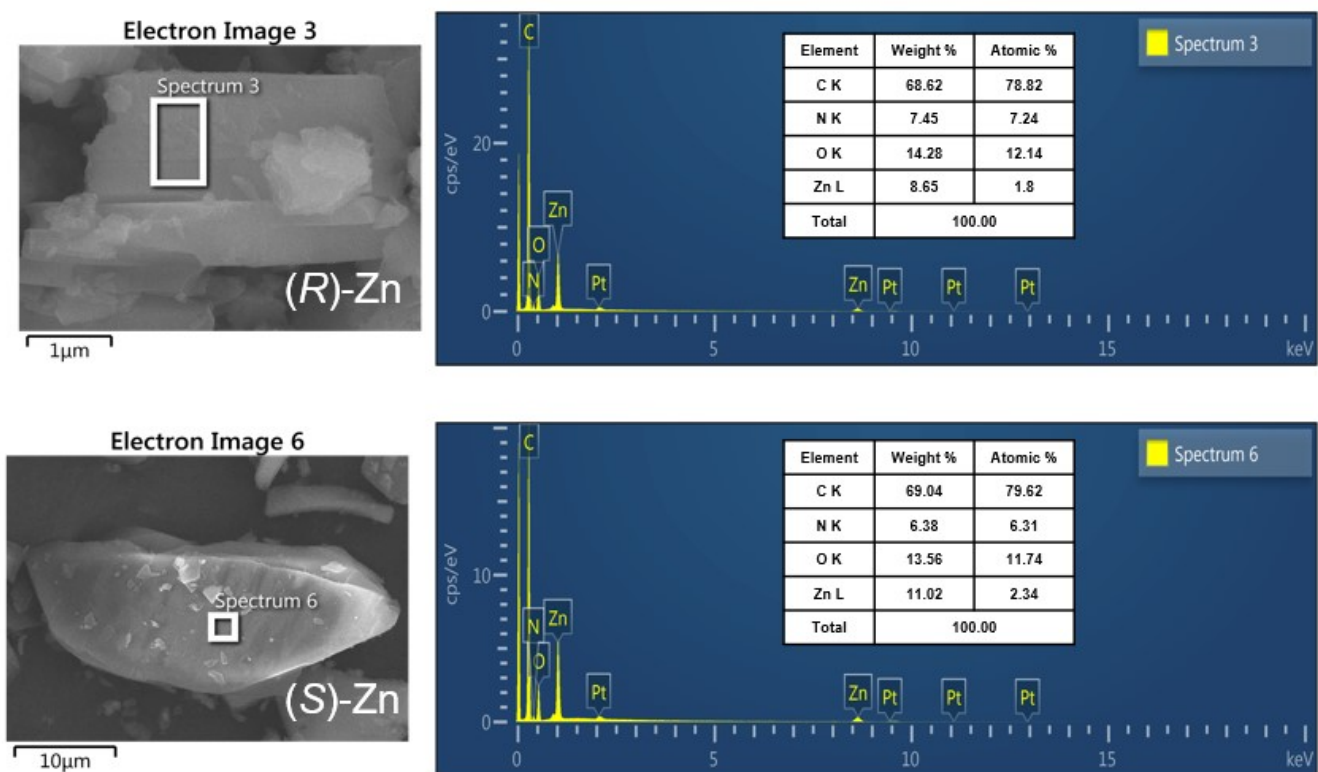


Fig. S5 IR spectra for (*R,R*)-TBPG, (*S,S*)-TBPG, (*R*)-Zn and (*S*)-Zn

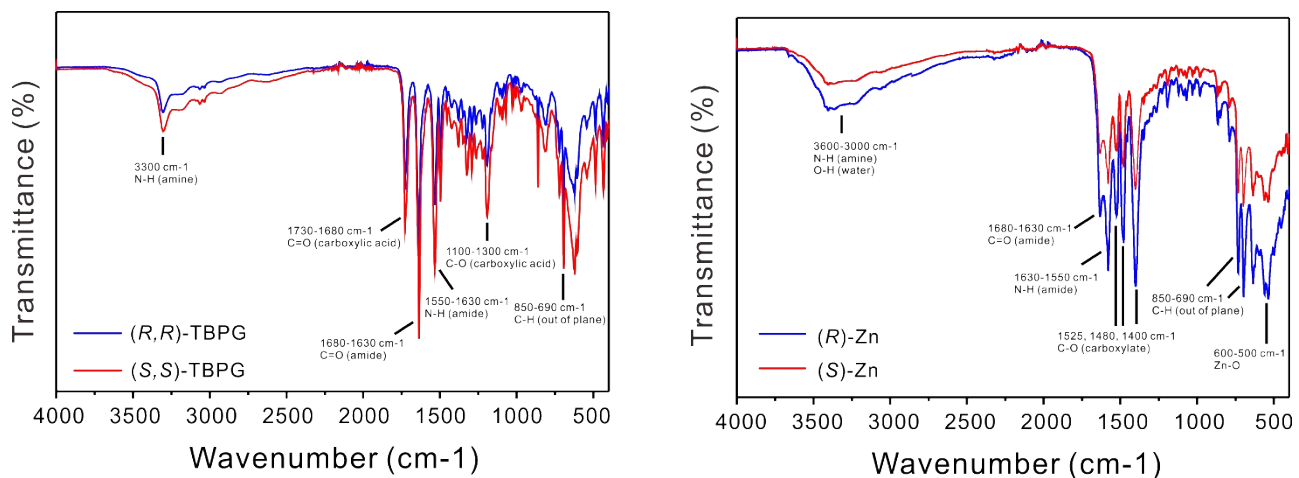


Fig. S6 UV-vis diffuse reflectance spectra for (R,R) -TBPB, (S,S) -TBPB, (R) -Zn and (S) -Zn

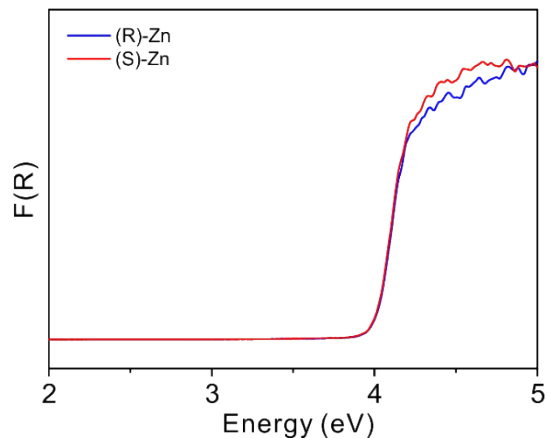
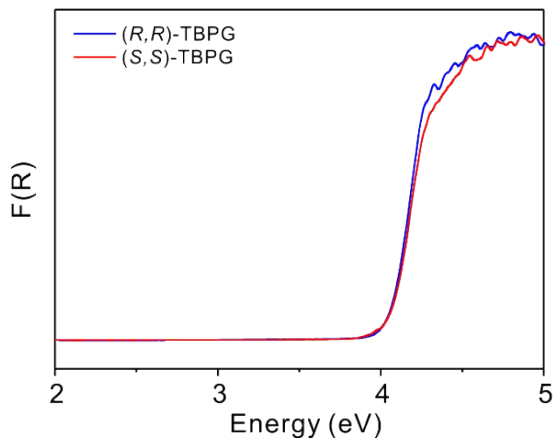
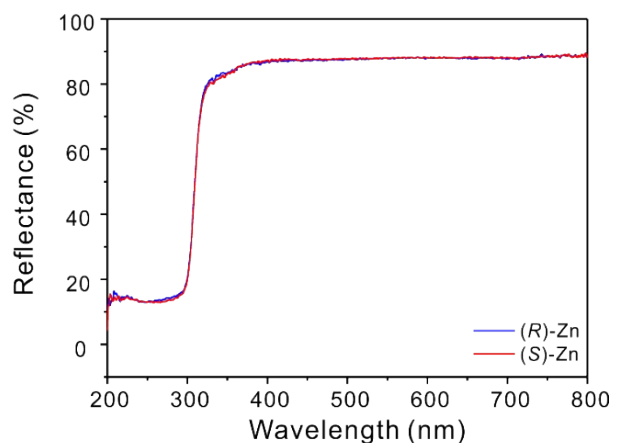
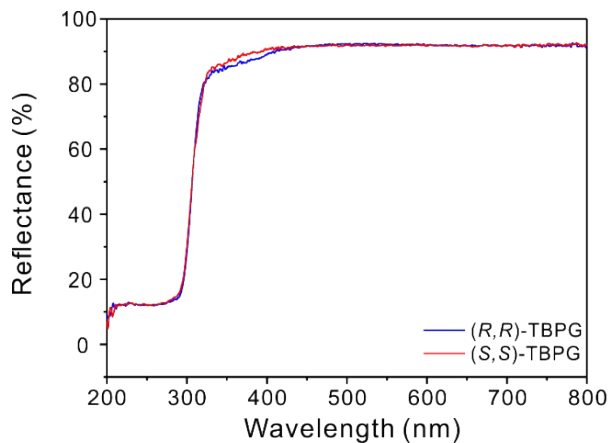


Fig. S7 TGA diagrams for (*R*)-Zn and (*S*)-Zn

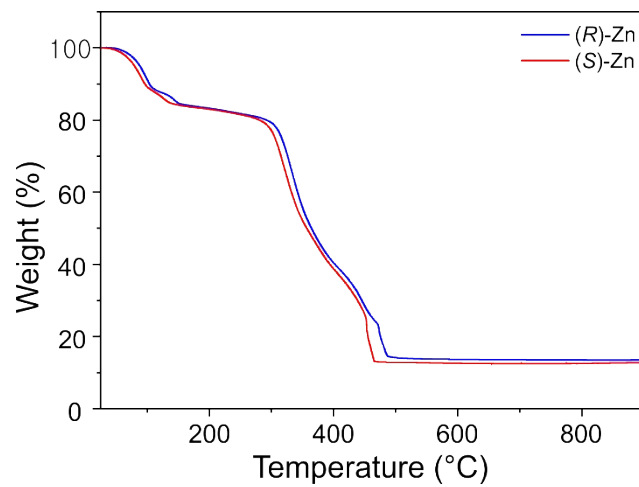


Fig. S8 PXRD patterns measured after heating the samples to 800 °C

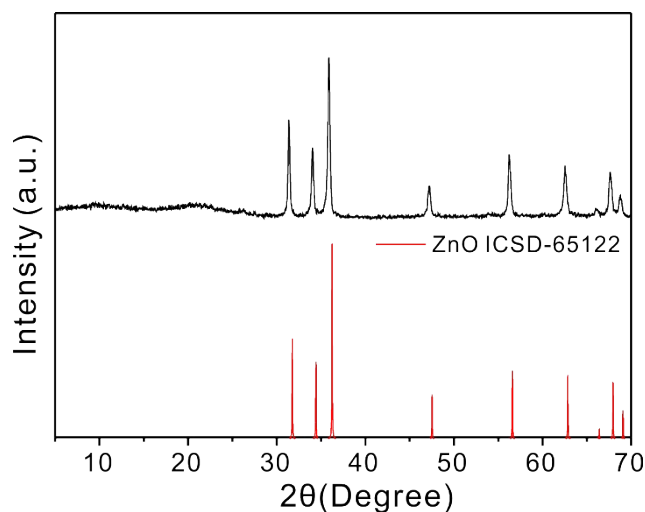


Fig. S9 (a) Solid-state CD spectra of (R,R) -TBPB, (S,S) -TBPB, (R) -Zn, and (S) -Zn. (b) Absorbance spectra of (R,R) -TBPB and (R) -Zn.

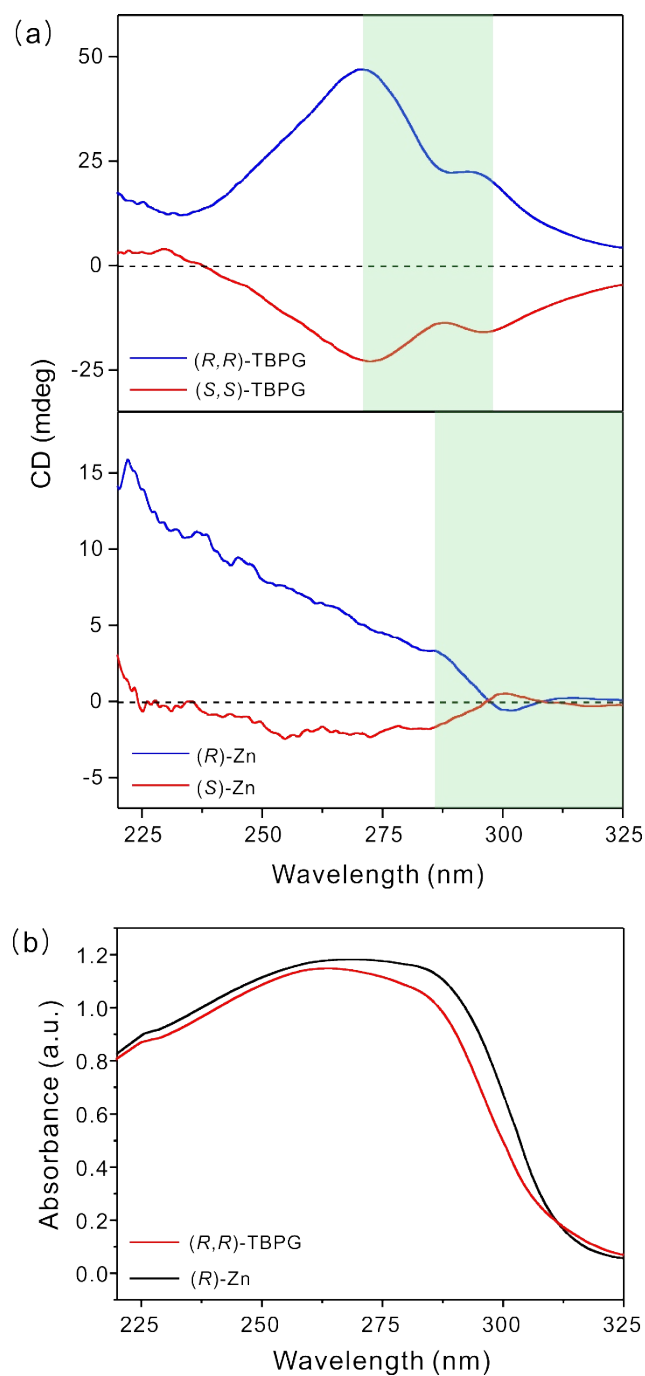


Fig. S10 Band structures for (a) (R)-Zn and (b) (S)-Zn. Arrows represent the optical transition from the valence band maximum to the conduction band minimum.

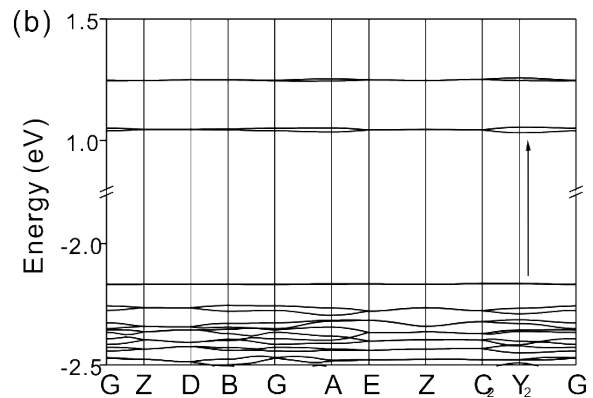
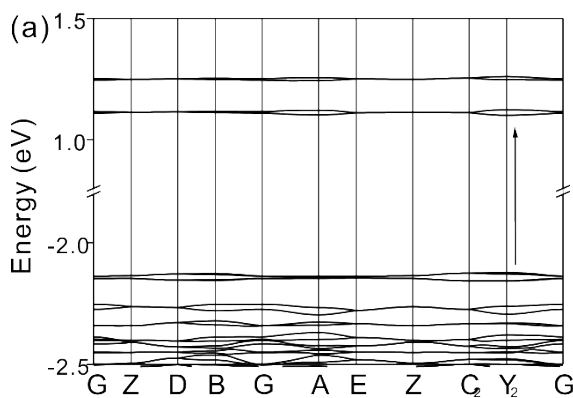


Fig. S11 Total and partial density of states for (a) (R)-Zn and (b) (S)-Zn

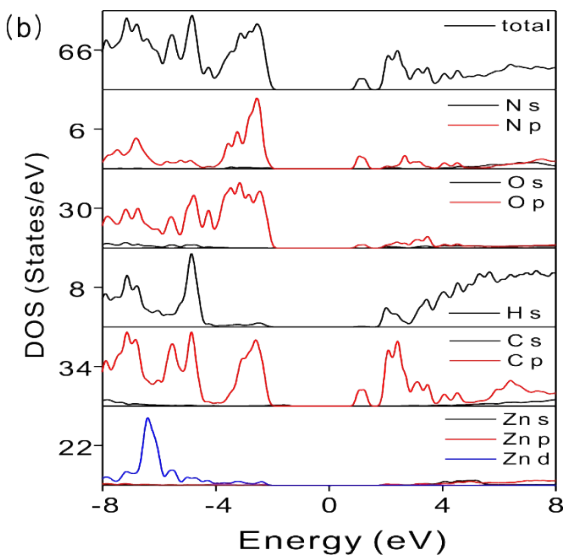
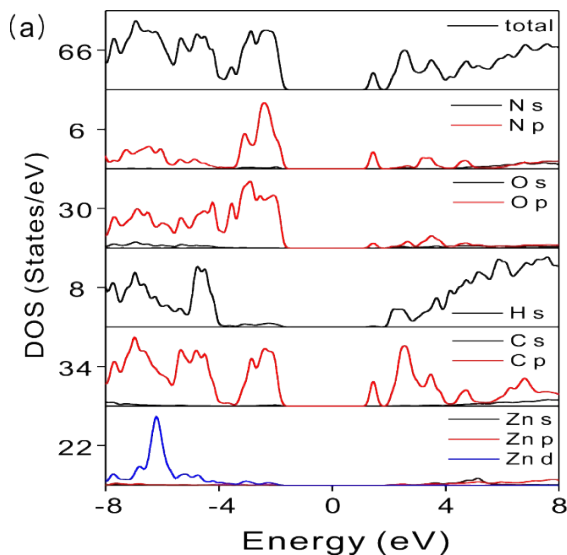


Fig. S12 Plots of SHG intensity versus particle size for (*R*)-Zn and (*S*)-Zn

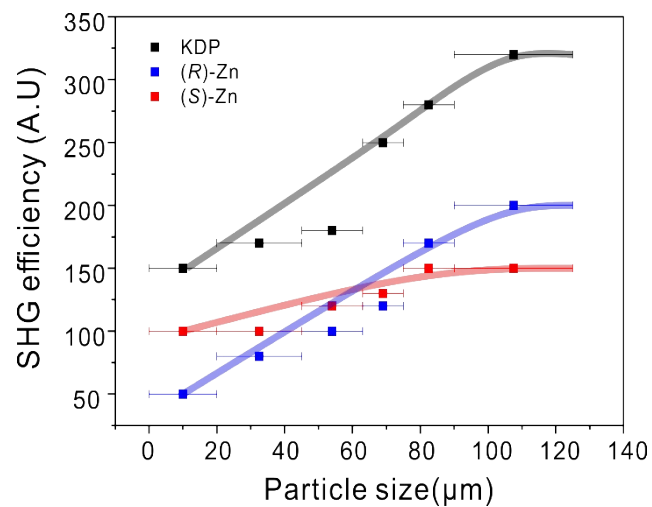


Table S6 Dipole moments for polyhedra in (R)-Zn and (S)-Zn

Compound	Unit	Magnitude	Dipole moment (D)		
			x	y	z
(R)-Zn	ZnO ₆ (1)	3.71 D	-1.01	3.57	-0.06
	ZnO ₆ (2)	2.93 D	-0.05	-2.63	-1.28
	ZnO ₆ (3)	3.71 D	1.01	3.57	0.06
	ZnO ₆ (4)	2.93 D	0.05	-2.63	1.28
	Net	1.87 D	0	1.87	0
(S)-Zn	ZnO ₆ (1)	2.85 D	-0.16	2.59	1.17
	ZnO ₆ (2)	3.62 D	0.82	-3.53	0.02
	ZnO ₆ (3)	2.85 D	0.16	2.59	-1.17
	ZnO ₆ (4)	3.62 D	-0.82	-3.53	-0.02
	Net	1.87 D	0	-1.87	0

Fig. S13 Net moments and dipole moments of ZnO₆ polyhedra in a unit cell

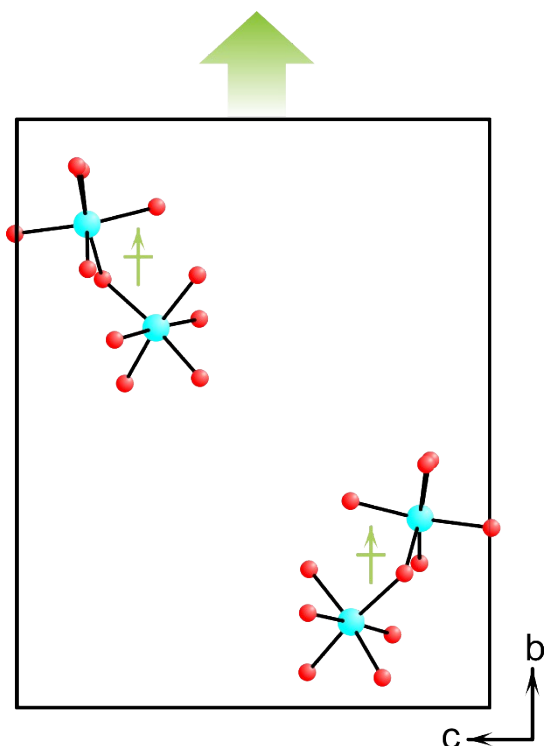


Fig. S14 PXRD patterns revealing the stability of (*R*)-Zn (a) in various solvents and (b) at various pH values.

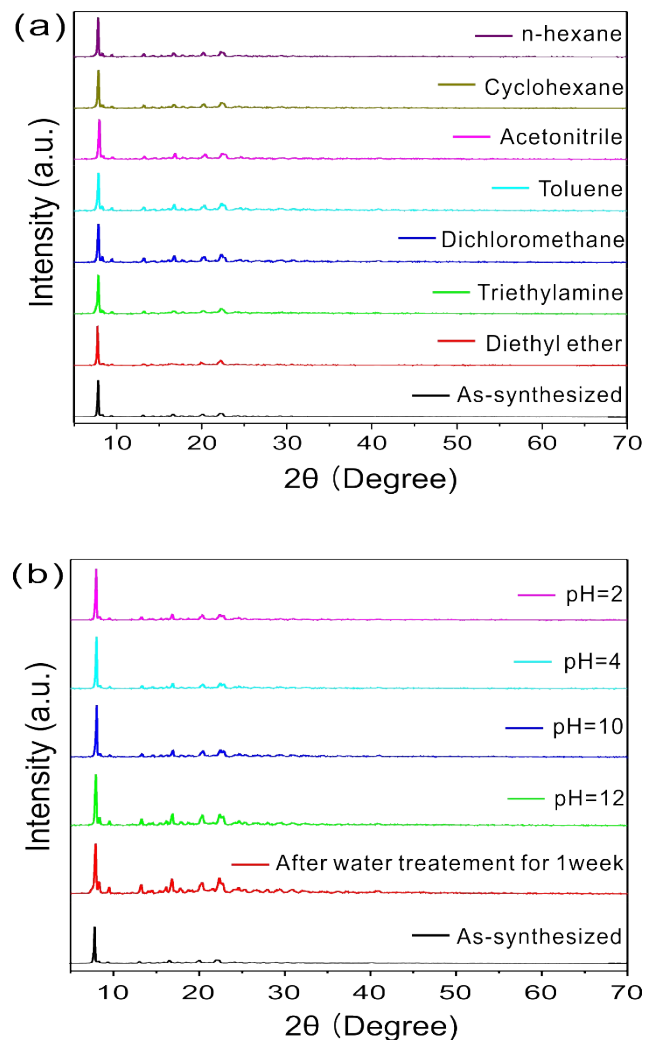


Table S7 Crystallographic Data for (S)-Zn-EtOH

(S)-Zn-EtOH	
fw	1178.72
space group	$P2_1$
a (Å)	12.177(2)
b (Å)	16.612(3)
c (Å)	14.691(3)
β (°)	114.36(3)
V (Å ³)	2707.2(11)
Z	2
T (K)	100(2)
λ (Å)	0.630
ρ_{calcd} (g/cm ³)	1.446
$R(F_o)^a$	0.0532
$R_w(F_o^2)^b$	0.0911
Flack x	0.023(9)

$$^aR(F) = \sum | |F_o| - |F_c| | / \sum |F_o|. \quad ^bR_w(F_o^2) = [\sum w(F_o^2 - F_c^2)^2 / \sum w(F_o^2)^2]^{1/2}.$$

Table S8 Selected bond distances (Å) and selected bond angles (°) for (S)-Zn-EtOH

Selected bond distances (Å)						
Zn(1)-O(4)	2.030(4)	O(4)-C(1)	1.254(6)	O(20)-C(49)	1.500(18)	C(41)-C(48)
Zn(1)-O(17)#1	2.057(4)	O(5)-C(1)	1.249(7)	C(1)-C(2)	1.547(9)	C(49)-C(50)
Zn(1)-O(13)#2	2.069(4)	O(6)-C(9)	1.232(6)	C(2)-C(3)	1.514(9)	N(1)-C(9)
Zn(1)-O(1)	2.132(5)	O(7)-C(16)	1.231(7)	C(9)-C(10)	1.516(8)	N(1)-C(2)
Zn(1)-O(3)	2.135(4)	O(8)-C(24)	1.258(7)	C(13)-C(16)	1.495(8)	N(2)-C(16)
Zn(1)-O(2)	2.157(5)	O(9)-C(24)	1.247(6)	C(17)-C(18)	1.533(9)	N(2)-C(17)
Zn(2)-O(12)#3	2.029(4)	O(12)-C(48)	1.270(7)	C(17)-C(24)	1.529(8)	N(3)-C(33)
Zn(2)-O(16)	2.052(4)	O(13)-C(48)	1.244(7)	C(25)-C(26)	1.578(8)	N(3)-C(26)
Zn(2)-O(9)	2.060(4)	O(14)-C(33)	1.235(8)	C(26)-C(27)	1.44(4)	N(4)-C(40)
Zn(2)-O(10)	2.073(4)	O(15)-C(40)	1.233(7)	C(33)-C(34)	1.498(8)	N(4)-C(41)
Zn(2)-O(2)#4	2.181(4)	O(16)-C(25)	1.261(7)	C(37)-C(40)	1.501(8)	
Zn(2)-O(11)	2.231(5)	O(17)-C(25)	1.256(7)	C(41)-C(42)	1.532(9)	
Selected bond angles (°)						
O(1)-Zn(1)-O(2)	89.10(19)	O(16)-Zn(2)-O(11)	173.87(17)	O(5)-C(1)-C(2)	117.4(5)	
O(1)-Zn(1)-O(3)	84.37(19)	O(17)#1-Zn(1)-O(1)	91.75(18)	O(6)-C(9)-C(10)	120.3(5)	
O(2)#4-Zn(2)-O(11)	89.76(18)	O(17)#1-Zn(1)-O(2)	88.95(16)	O(7)-C(16)-C(13)	120.9(5)	
O(3)-Zn(1)-O(2)	92.63(17)	O(17)#1-Zn(1)-O(3)	175.79(17)	O(8)-C(24)-C(17)	116.6(5)	
O(4)-Zn(1)-O(1)	85.10(19)	O(17)#1-Zn(1)-O(13)#2	96.90(17)	O(9)-C(24)-C(17)	116.2(5)	
O(4)-Zn(1)-O(2)	172.29(17)	Zn(1)-O(2)-Zn(2)#2	111.6(2)	O(12)-C(48)-C(41)	115.4(5)	
O(4)-Zn(1)-O(3)	91.97(17)	C(1)-O(4)-Zn(1)	130.2(4)	O(13)-C(48)-C(41)	118.2(5)	
O(4)-Zn(1)-O(13)#2	91.74(15)	C(24)-O(9)-Zn(2)	128.1(4)	O(14)-C(33)-C(34)	121.4(5)	
O(4)-Zn(1)-O(17)#1	86.05(16)	C(25)-O(16)-Zn(2)	134.5(4)	O(16)-C(25)-C(26)	116.6(5)	
O(9)-Zn(2)-O(2)#4	172.51(16)	C(25)-O(17)-Zn(1)#4	133.0(4)	O(17)-C(25)-C(26)	117.5(6)	
O(9)-Zn(2)-O(10)	92.12(17)	C(48)-O(12)-Zn(2)#5	132.8(4)	O(20)-C(49)-C(50)	111.2(11)	
O(9)-Zn(2)-O(11)	84.03(18)	C(48)-O(13)-Zn(1)#6	133.2(4)	N(1)-C(2)-C(3)	113.6(5)	
O(10)-Zn(2)-O(2)#4	91.47(17)	O(5)-C(1)-O(4)	130.2(4)	N(1)-C(2)-C(1)	109.9(5)	
O(10)-Zn(2)-O(11)	84.81(18)	O(8)-C(24)-O(9)	127.2(6)	N(1)-C(9)-C(10)	116.9(5)	
O(12)#3-Zn(2)-O(2)#4	87.76(16)	O(13)-C(48)-O(12)	126.5(5)	N(2)-C(16)-C(13)	117.9(5)	
O(12)#3-Zn(2)-O(9)	87.65(16)	O(17)-C(25)-O(16)	125.9(6)	N(2)-C(17)-C(18)	112.8(5)	
O(12)#3-Zn(2)-O(10)	170.86(18)	O(6)-C(9)-N(1)	122.7(5)	N(2)-C(17)-C(24)	109.6(5)	
O(12)#3-Zn(2)-O(11)	86.08(17)	O(7)-C(16)-N(2)	121.2(5)	N(3)-C(26)-C(27)	111.4(17)	
O(12)-Zn(2)-O(16)#3	98.36(17)	O(14)-C(33)-N(3)	121.5(5)	N(3)-C(26)-C(25)	108.3(5)	
O(13)#2-Zn(1)-O(1)	170.58(18)	O(15)-C(40)-N(4)	121.6(5)	N(3)-C(33)-C(34)	117.2(6)	
O(13)#2-Zn(1)-O(2)	94.69(17)	C(9)-N(1)-C(2)	121.3(5)	N(4)-C(40)-C(37)	117.6(5)	
O(13)#2-Zn(1)-O(3)	86.87(17)	C(16)-N(2)-C(17)	120.0(5)	N(4)-C(41)-C(42)	112.6(5)	
O(16)-Zn(2)-O(2)#4	94.61(17)	C(33)-N(3)-C(26)	123.1(5)	N(4)-C(41)-C(48)	109.9(5)	
O(16)-Zn(2)-O(9)	91.91(17)	C(40)-N(4)-C(41)	121.2(5)			
O(16)-Zn(2)-O(10)	90.78(17)	O(4)-C(1)-C(2)	115.8(5)			

Symmetry operation : #1 x-1,y-1,z-1 #2 x,y-1,z #3 x-1,y,z-1 #4 x,y+1,z #5 x+1,y,z+1 #6 x+1,y+1,z+1

Table S9 Hydrogen bonds distances (\AA) for (S)-Zn-EtOH

D-H...A	d(D...A)	D-H...A	d(D...A)
N(1)-H(1)...O(18)#1	2.974(6)	O(18)-H(1D)...O(8)#8	2.857(6)
O(1)-H(10)...O(15)#7	2.717(6)	O(18)-H(1E)...O(17)	2.835(6)
O(1)-H(13)...O(3)	2.865(6)	O(18)-H(1E)...O(4)#4	3.000(6)
O(2)-H(9)...O(21)	2.566(7)	O(19)-H(1H)...O(12)	2.751(6)
O(3)-H(16)...O(5)	2.714(4)	O(19)-H(1F)...O(5)#8	2.839(6)
O(3)-H(1G)...O(6)#9	2.809(6)	O(21)-H(1B)...O(6)#9	2.744(7)
O(10)-H(1L)...O(7)#8	2.732(6)	C(50)-H(50A)...O(14)#7	2.779(8)
O(10)-H(1M)...O(8)	2.635(6)	O(50)-H(50B)...O(11)	2.755(8)
O(11)-H(1N)...O(19)#3	2.825(8)		

Symmetry operation : #1 x-1,y-1,z-1 #3 x,y,z-1 #4 x,y-1,z #7 -x,y+1/2,-z
#7 -x+1,y+1/2,-z+1 #8 -x+1,y+1/2,-z+1 #9 -x,y-1/2,-z

Fig. S15 Experimental and calculated powder X-ray diffraction patterns of (S)-Zn-EtOH

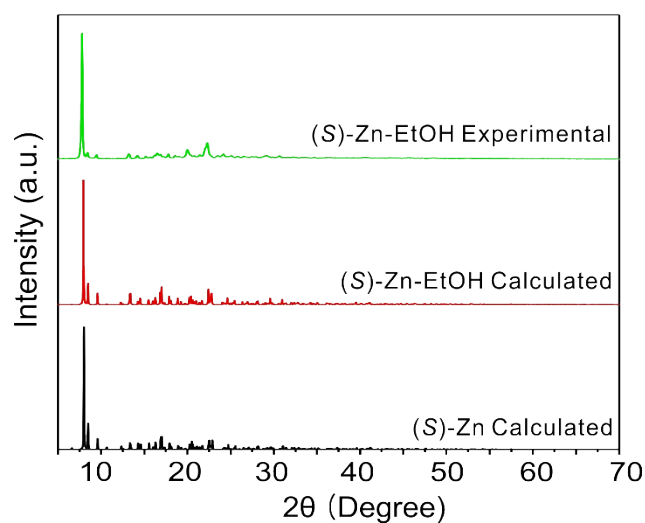
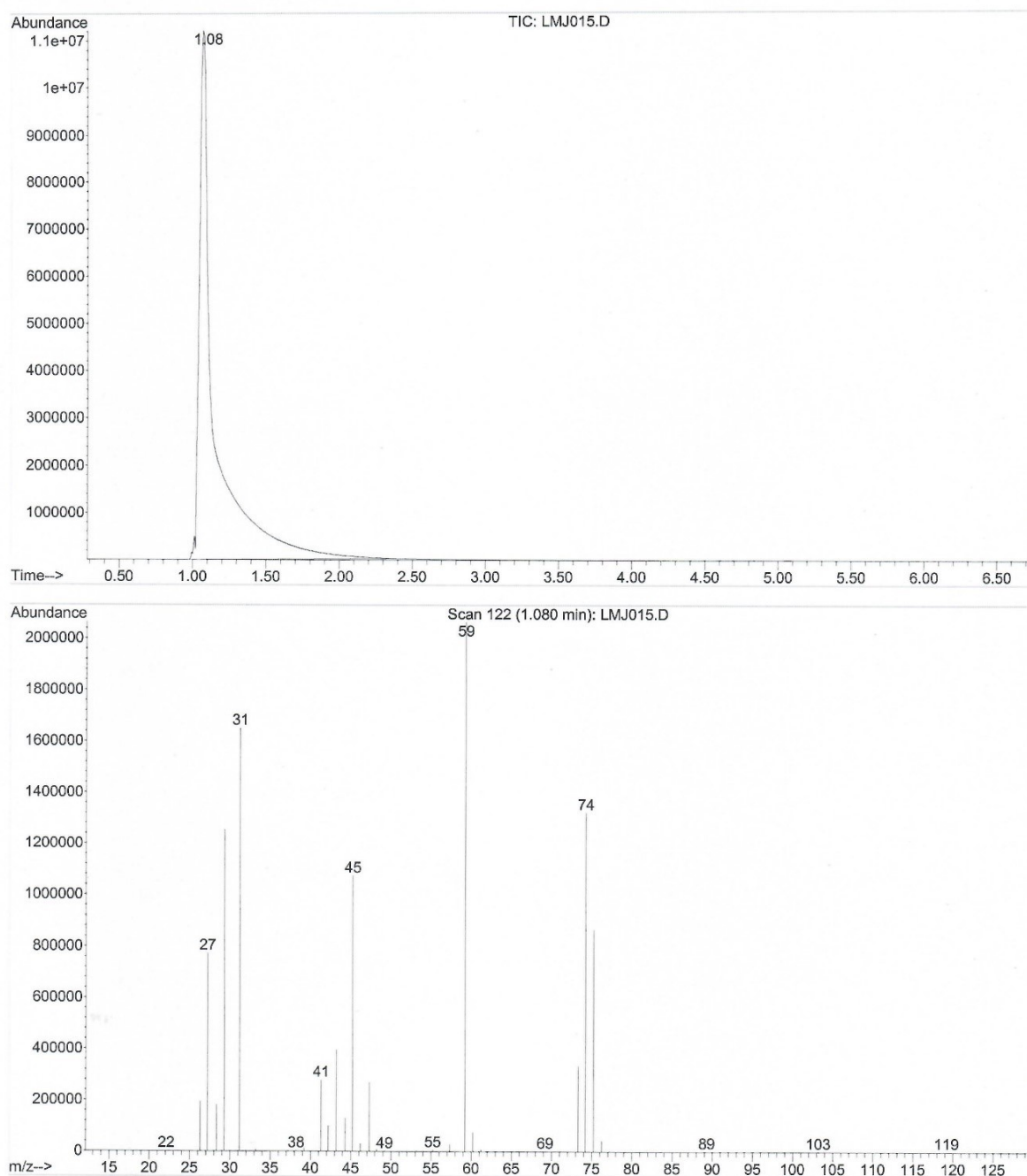


Fig. S16 GC-MS result of distilled diethyl ether



Area Percent Report

Data File : C:\MSDCHEM\1\DATA\LMJ015.D Vial: 1
Acq On : 14 Dec 2021 11:03 Operator: LHK
Sample : LMJ D_Ether Inst : Instrumen
Misc : 60/10/10/240 Multiplr: 1.00
Sample Amount: 0.00

MS Integration Params: autoint1.e

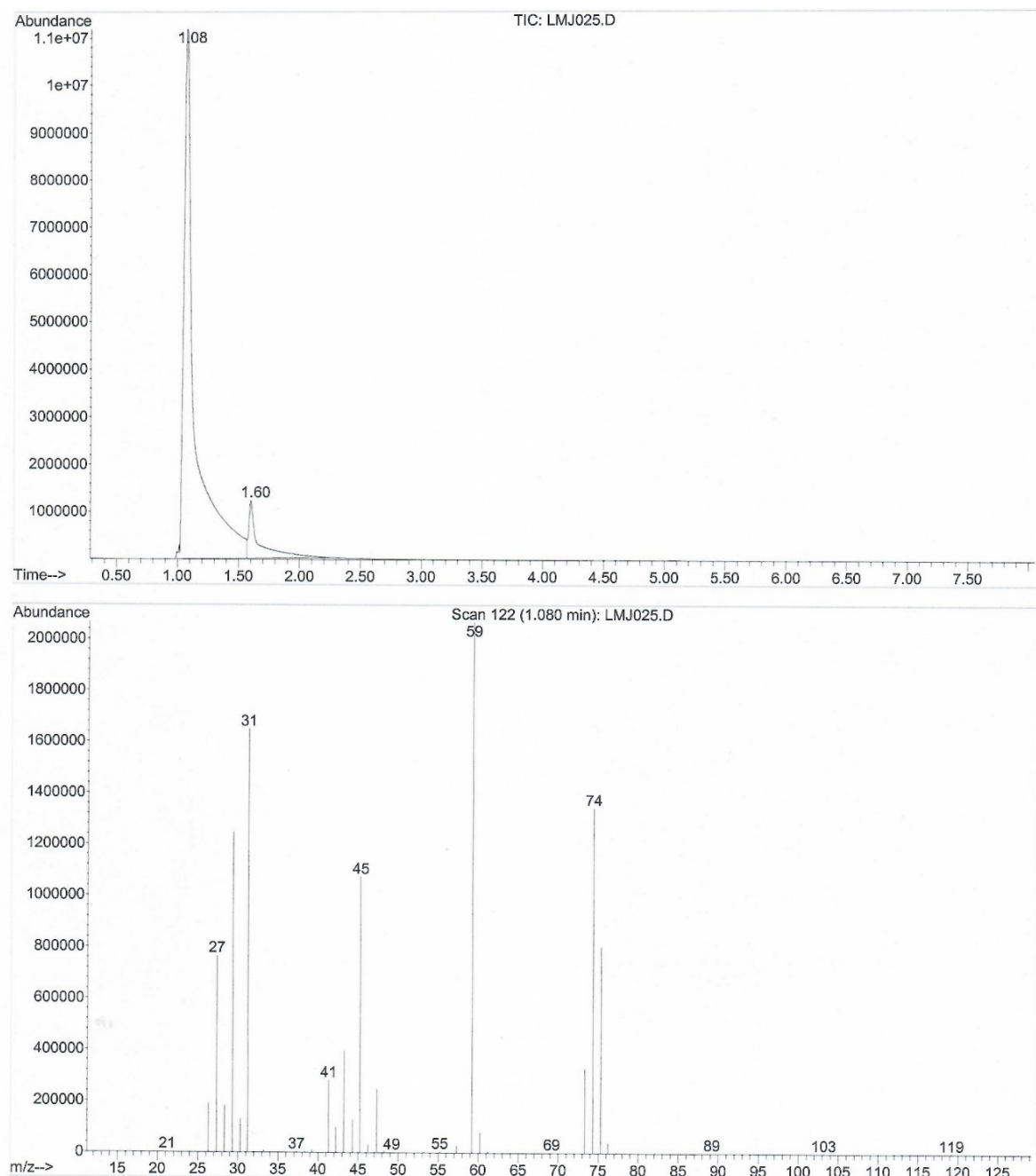
Method : C:\MSDCHEM\1\METHODS\DEFAULT.M (Chemstation Integrator)
Title :

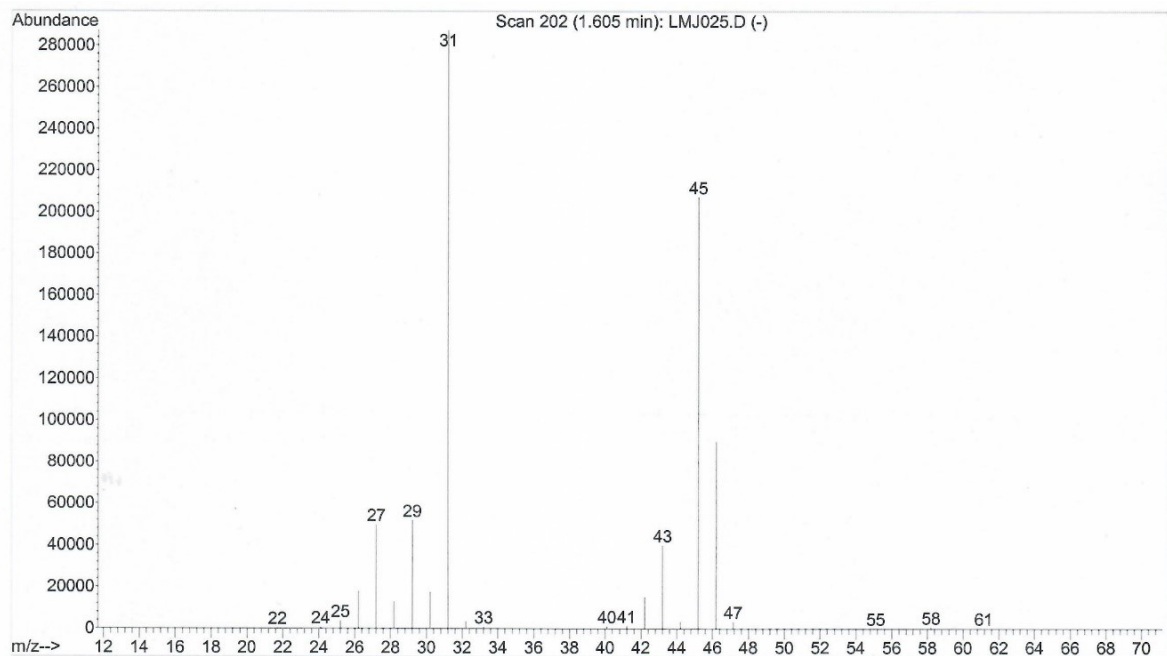
Signal : TIC

peak #	R.T. min	first scan	max scan	last scan	PK TY	peak height	corr. area	corr. % max.	% of total
1	1.080	105	122	330	BB 6	11191739	804600884	100.00%	100.000%

Sum of corrected areas: 804600884

Fig. S17 GC-MS result of distilled diethyl ether containing (*S*)-Zn crystal for 1 day





Area Percent Report

Data File : C:\MSDCHEM\1\DATA\LMJ025.D Vial: 1
 Acq On : 28 Dec 2021 14:26 Operator: LHK
 Sample : LMJ D_ether_1d Inst : Instrumen
 Misc : 60/10/10/240 Multiplr: 1.00
 Sample Amount: 0.00

MS Integration Params: autoint1.e

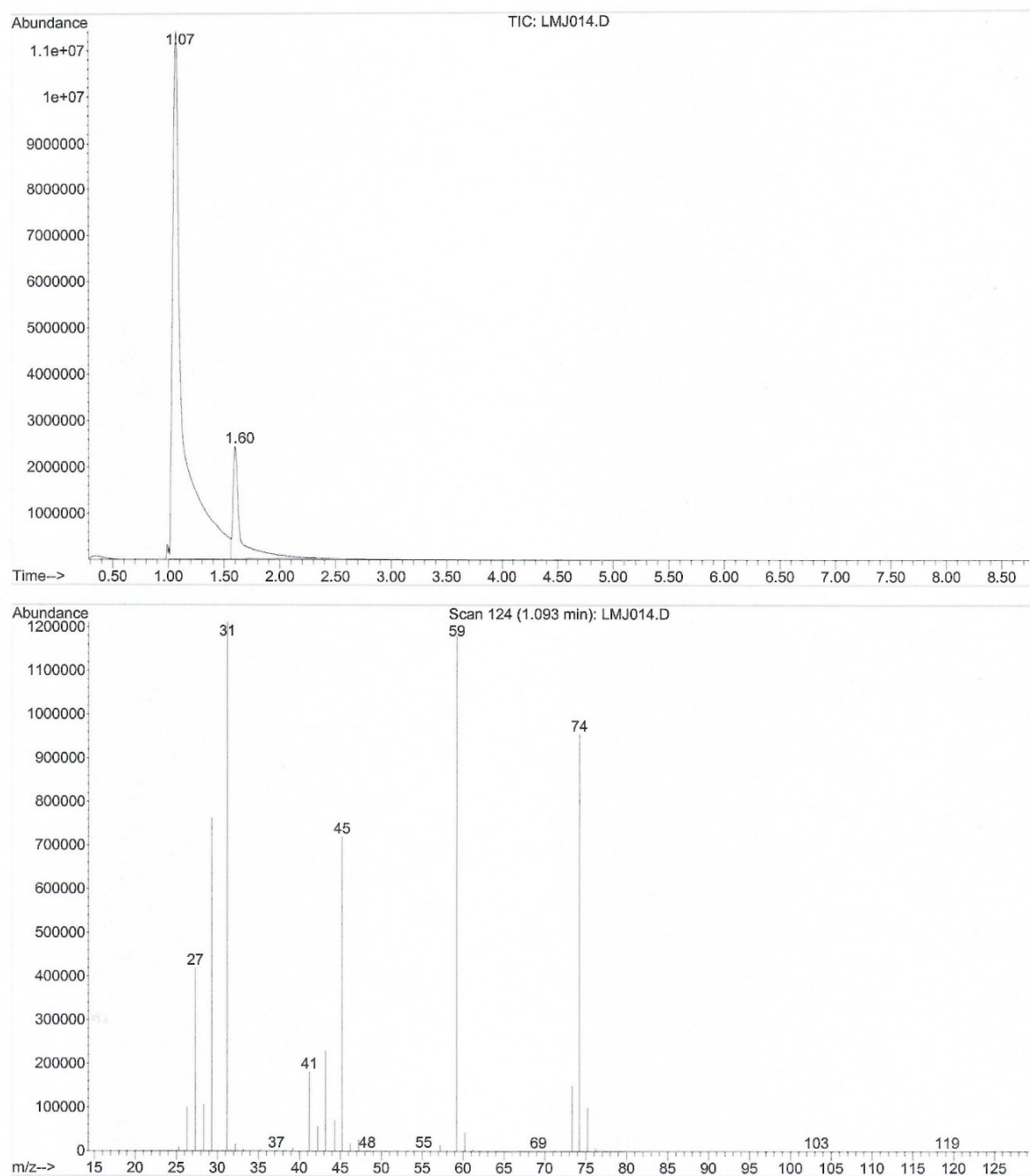
Method : C:\MSDCHEM\1\METHODS\DEFAULT.M (Chemstation Integrator)
 Title :

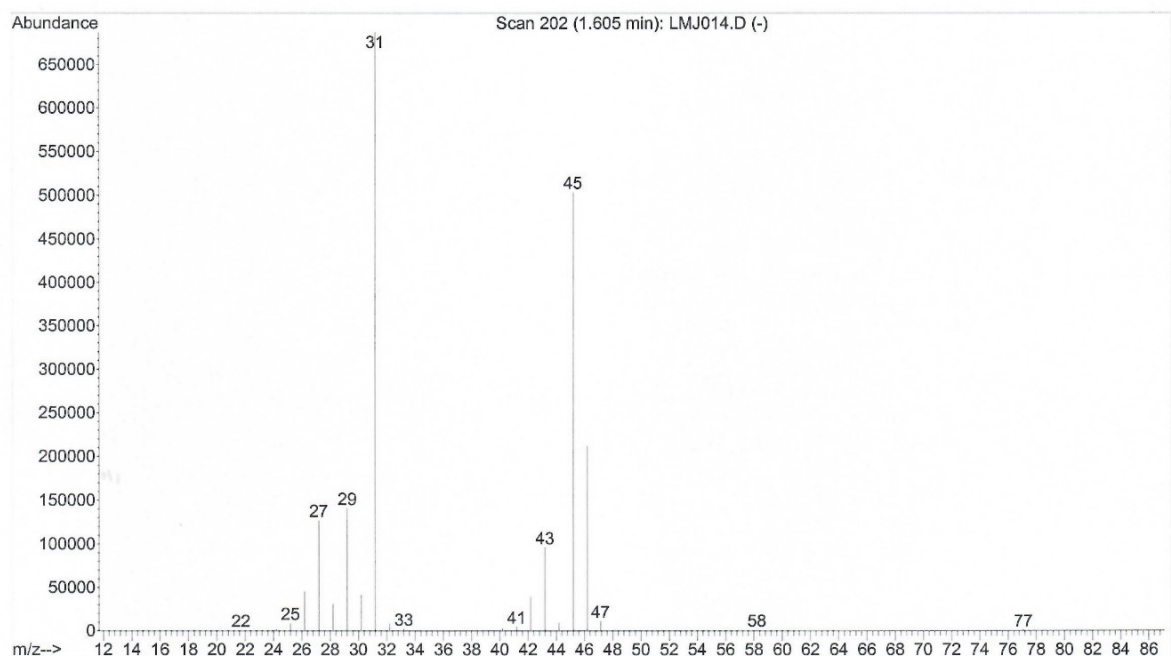
Signal : TIC

peak #	R.T. min	first scan	max scan	last scan	PK TY	peak height	corr. area	corr. % max.	% of total
1	1.080	105	122	196	BV 5	11189299	695965201	100.00%	90.552%
2	1.605	196	202	305	VB	1211433	72614507	10.43%	9.448%

Sum of corrected areas: 768579707

Fig. S18 GC-MS result of distilled diethyl ether containing (*S*)-Zn crystal for 3 days





Area Percent Report

Data File : C:\MSDCHEM\1\DATA\LMJ014.D Vial: 1
Acq On : 14 Dec 2021 10:44 Operator: LHK
Sample : LMJ_D_Ether_3d Inst : Instrumen
Misc : 60/10/10/240 Multiplr: 1.00
Sample Amount: 0.00

MS Integration Params: autoint1.e

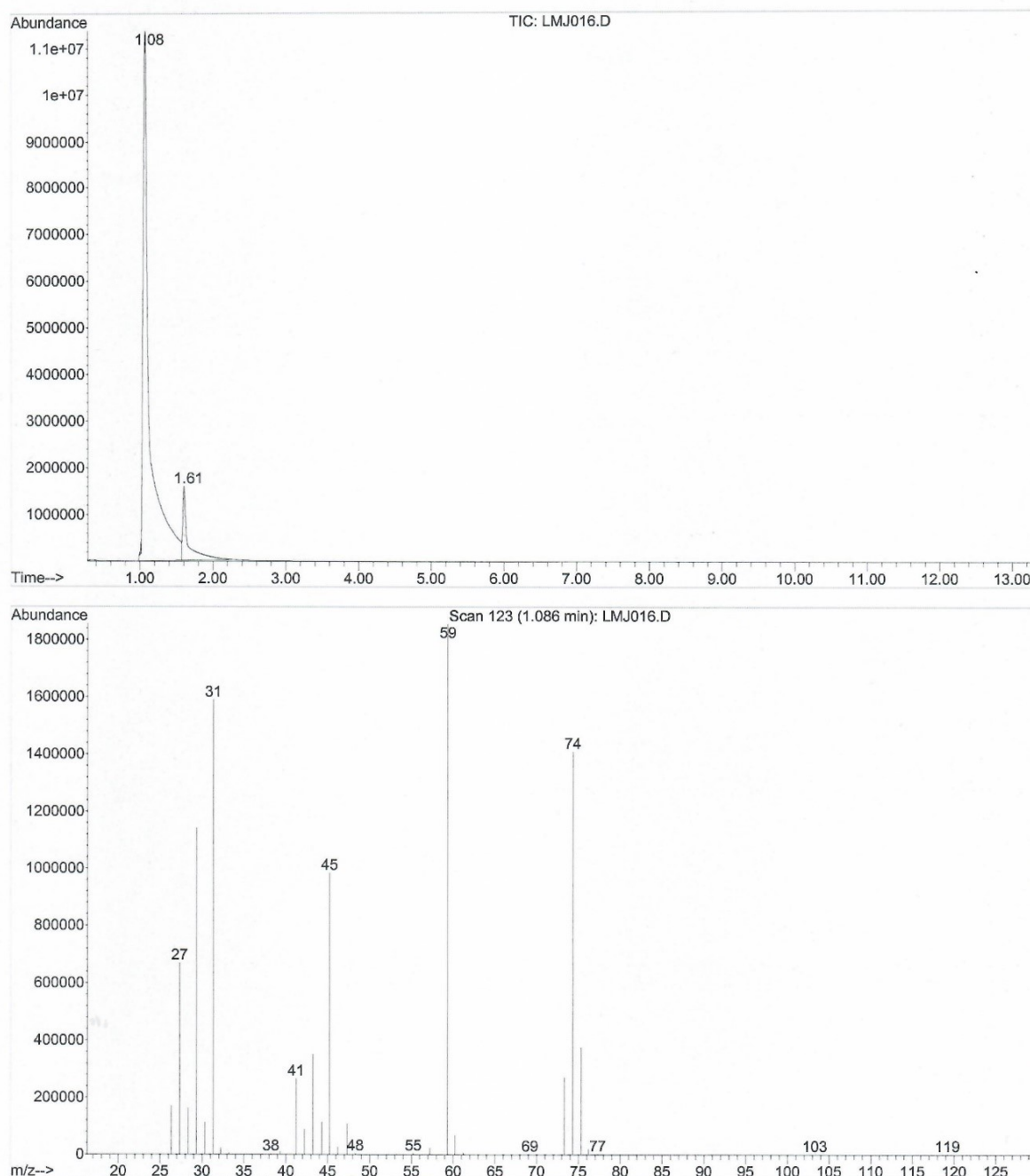
Method : C:\MSDCHEM\1\METHODS\DEFAULT.M (Chemstation Integrator)
Title :

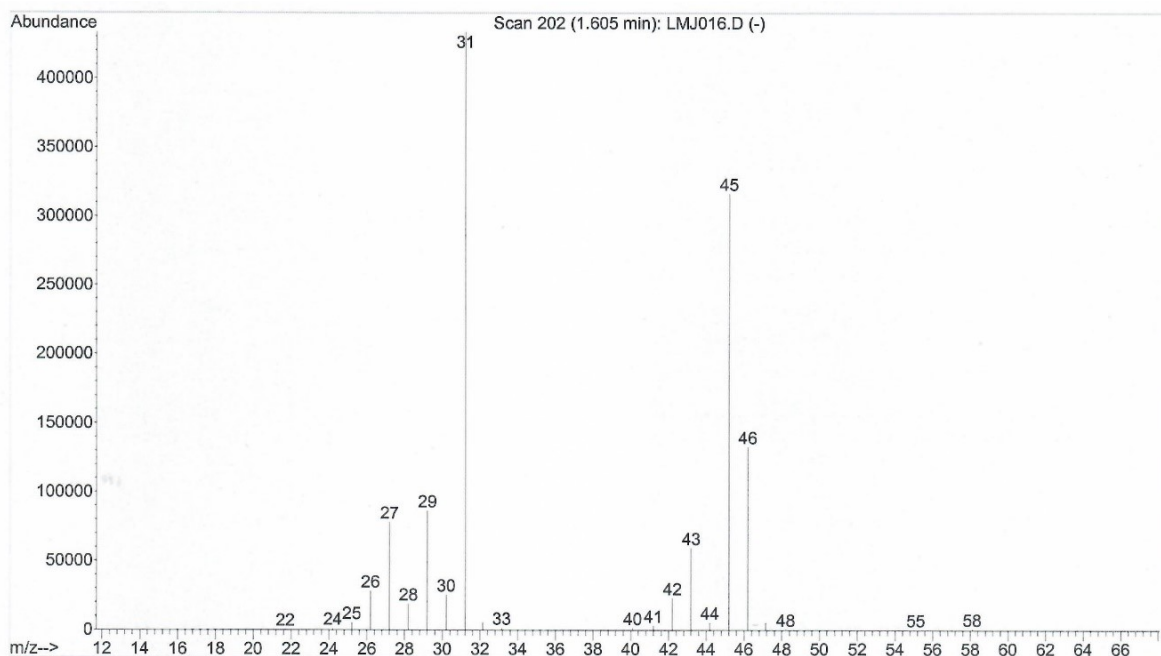
Signal : TIC

peak	R.T.	first	max	last	PK	peak	corr.	corr.	% of
#	min	scan	scan	scan	TY	height	area	% max.	total
1	1.073	94	121	195	BV 5	11343887	736637667	100.00%	86.393%
2	1.605	195	202	318	VB	2413252	116019525	15.75%	13.607%

Sum of corrected areas: 852657192

Fig. S19 GC-MS result of distilled diethyl ether containing (*S*)-Zn crystal for 7 days





Area Percent Report

```

Data File : C:\MSDCHEM\1\DATA\LMJ016.D           Vial: 1
Acq On    : 17 Dec 2021 10:28                  Operator: LHK
Sample     : LMJ D_ether_7d                    Inst   : Instrumen
Misc       : 60/10/10/240                     Multiplr: 1.00
                                                    Sample Amount: 0.00

```

MS Integration Params: autoint1.e

```

Method      : C:\MSDCHEM\1\METHODS\DEFAULT.M (Chemstation Integrator)
Title       :

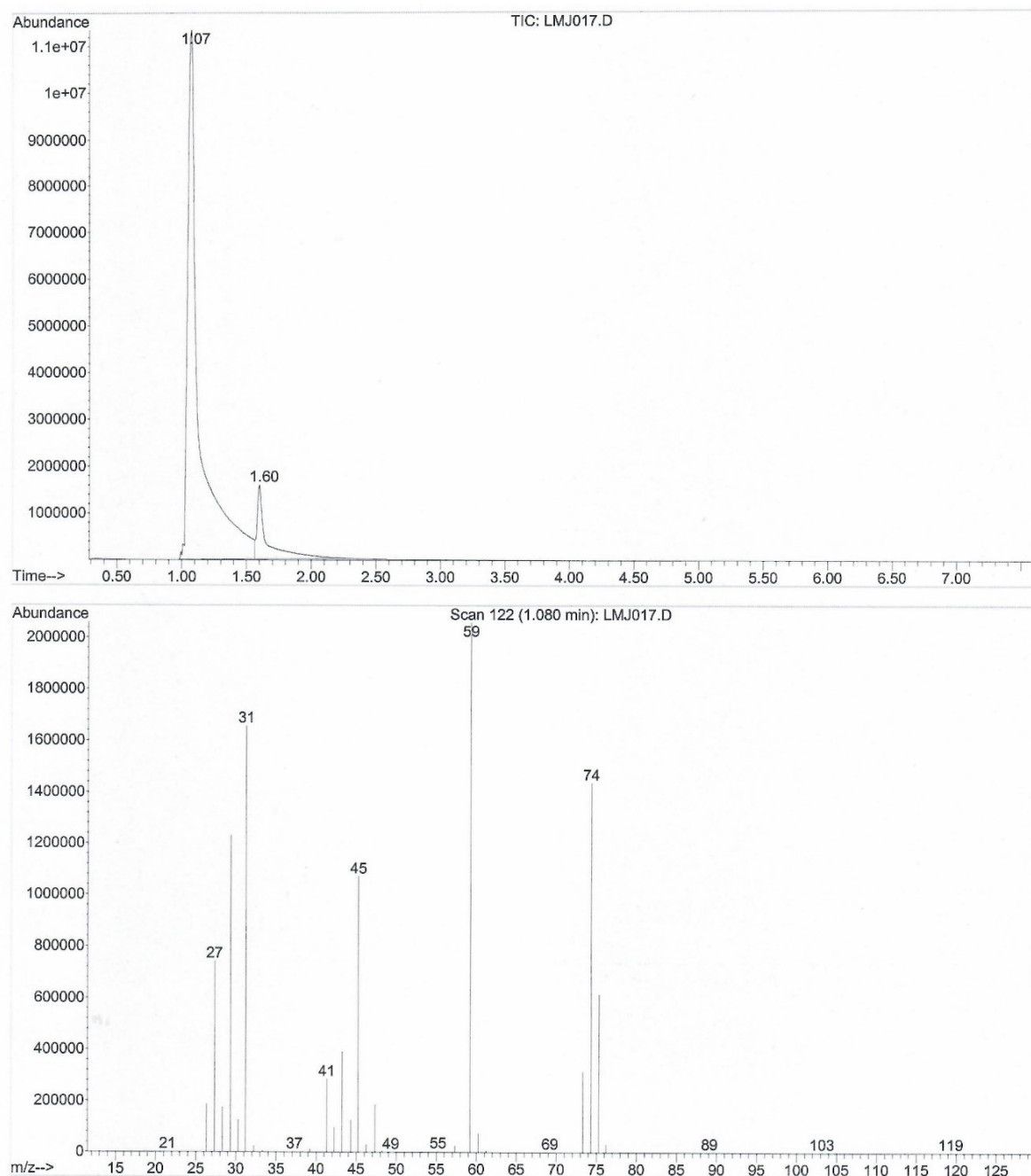
```

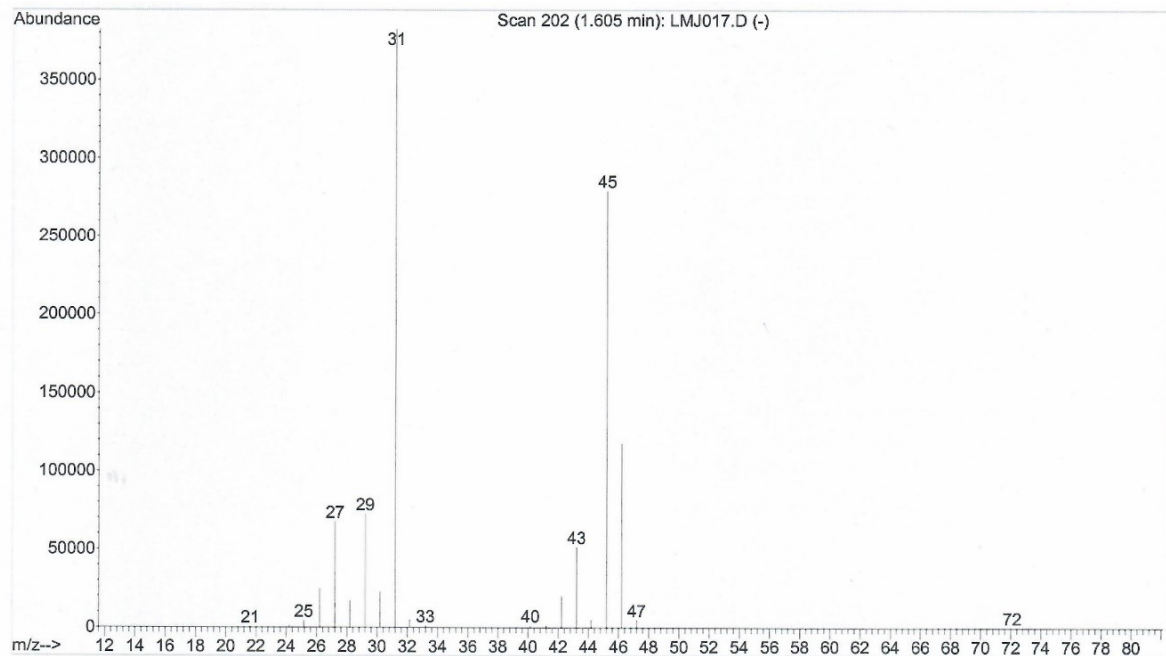
Signal : TIC

peak #	R.T. min	first scan	max scan	last scan	PK TY	peak height	corr. area	corr. % max.	% of total
1	1.073	95	121	196	BV 5	11372559	705957412	100.00%	89.595%
2	1.605	196	202	309	VB	1568131	81984419	11.61%	10.405%

Sum of corrected areas: 787941831

Fig. S20 GC-MS result of distilled diethyl ether containing (*S*)-Zn crystal for 10 days





Area Percent Report

Data File : C:\MSDCHEM\1\DATA\LMJ017.D Vial: 1
 Acq On : 20 Dec 2021 11:02 Operator: LHK
 Sample : LMJ_D_ether_10d Inst : Instrumen
 Misc : 60/10/10/240 Multiplr: 1.00
 Sample Amount: 0.00

MS Integration Params: autoint1.e

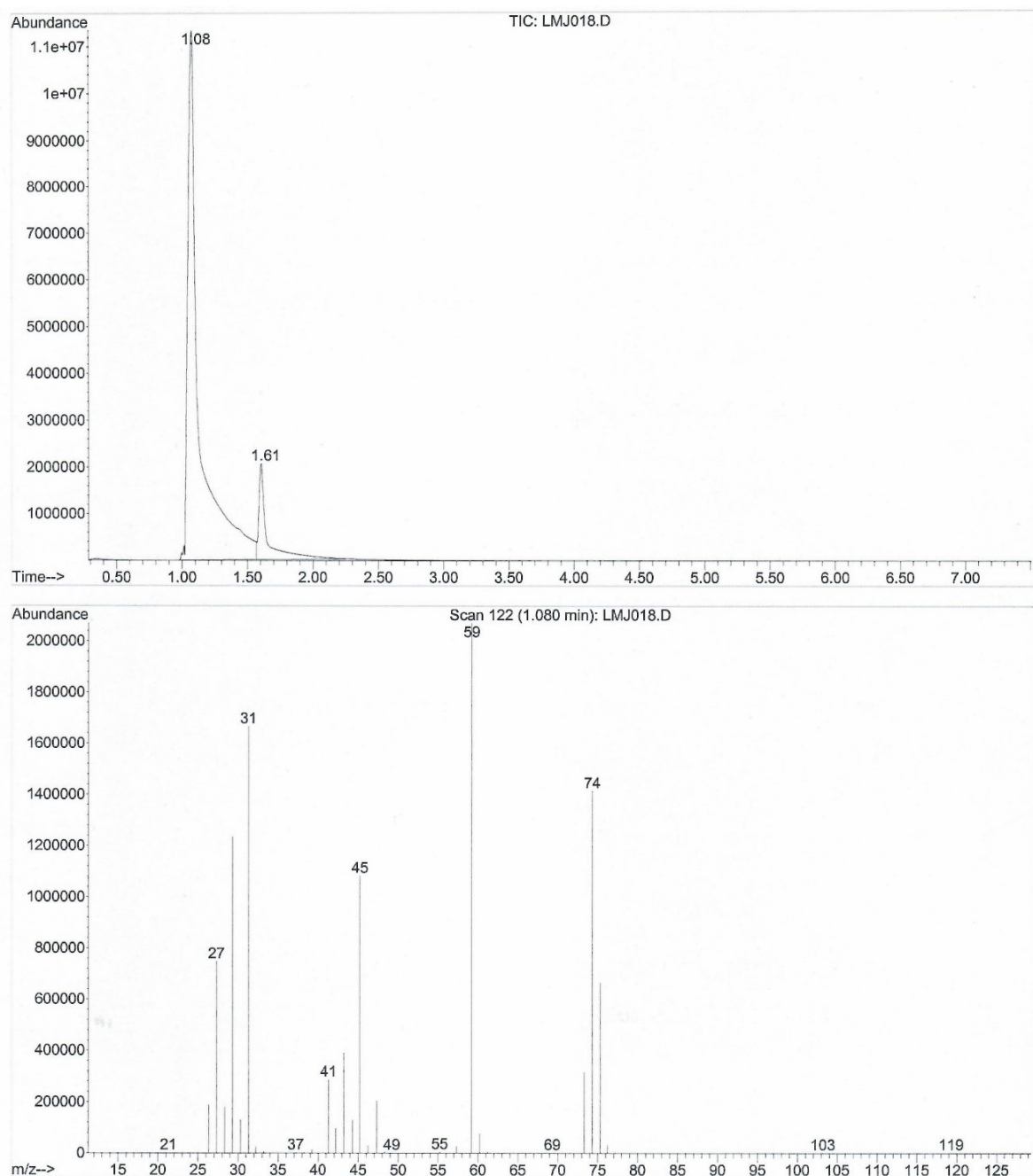
Method : C:\MSDCHEM\1\METHODS\DEFAULT.M (Chemstation Integrator)
 Title :

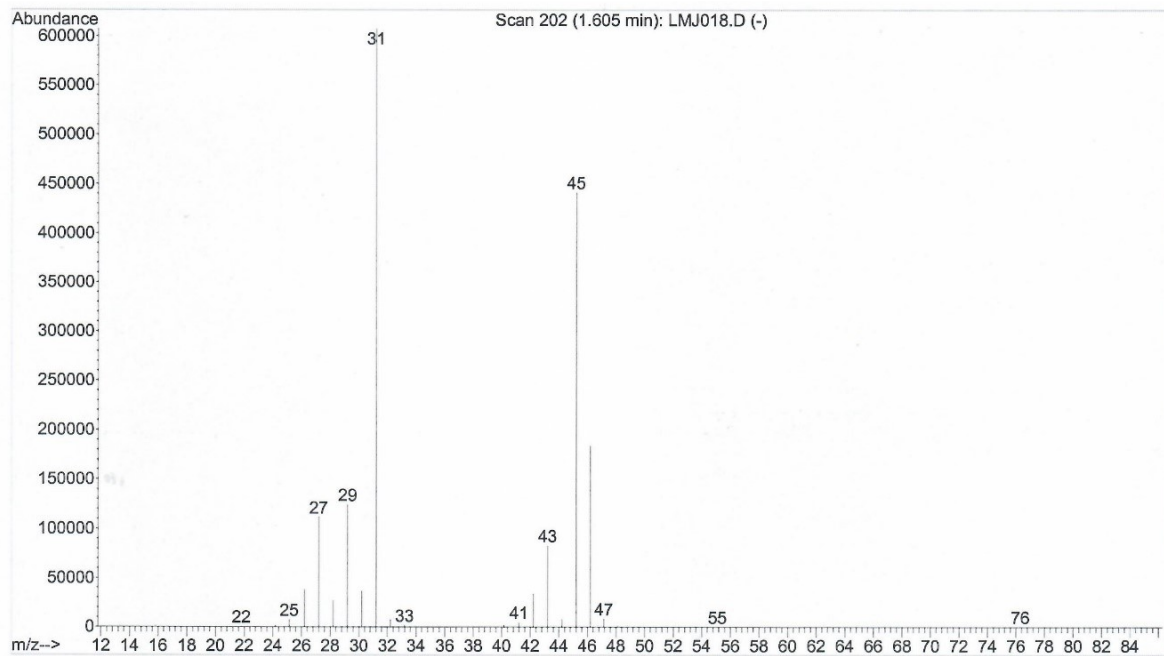
Signal : TIC

peak #	R.T. min	first scan	max scan	last scan	PK TY	peak height	corr. area	corr. % max.	% of total
1	1.073	95	121	196	BV 4	11295725	702351997	100.00%	89.354%
2	1.599	196	201	310	VB	1558770	83683504	11.91%	10.646%

Sum of corrected areas: 786035501

Fig. S21 GC-MS result of distilled diethyl ether containing (*S*)-Zn crystal for 14 days





Area Percent Report

Data File : C:\MSDCHEM\1\DATA\LMJ018.D Vial: 1
 Acq On : 24 Dec 2021 13:59 Operator: LHK
 Sample : LMJ D_ether_14d Inst : Instrumen
 Misc : 60/10/10/240 Multiplr: 1.00
 Sample Amount: 0.00

MS Integration Params: autoint1.e

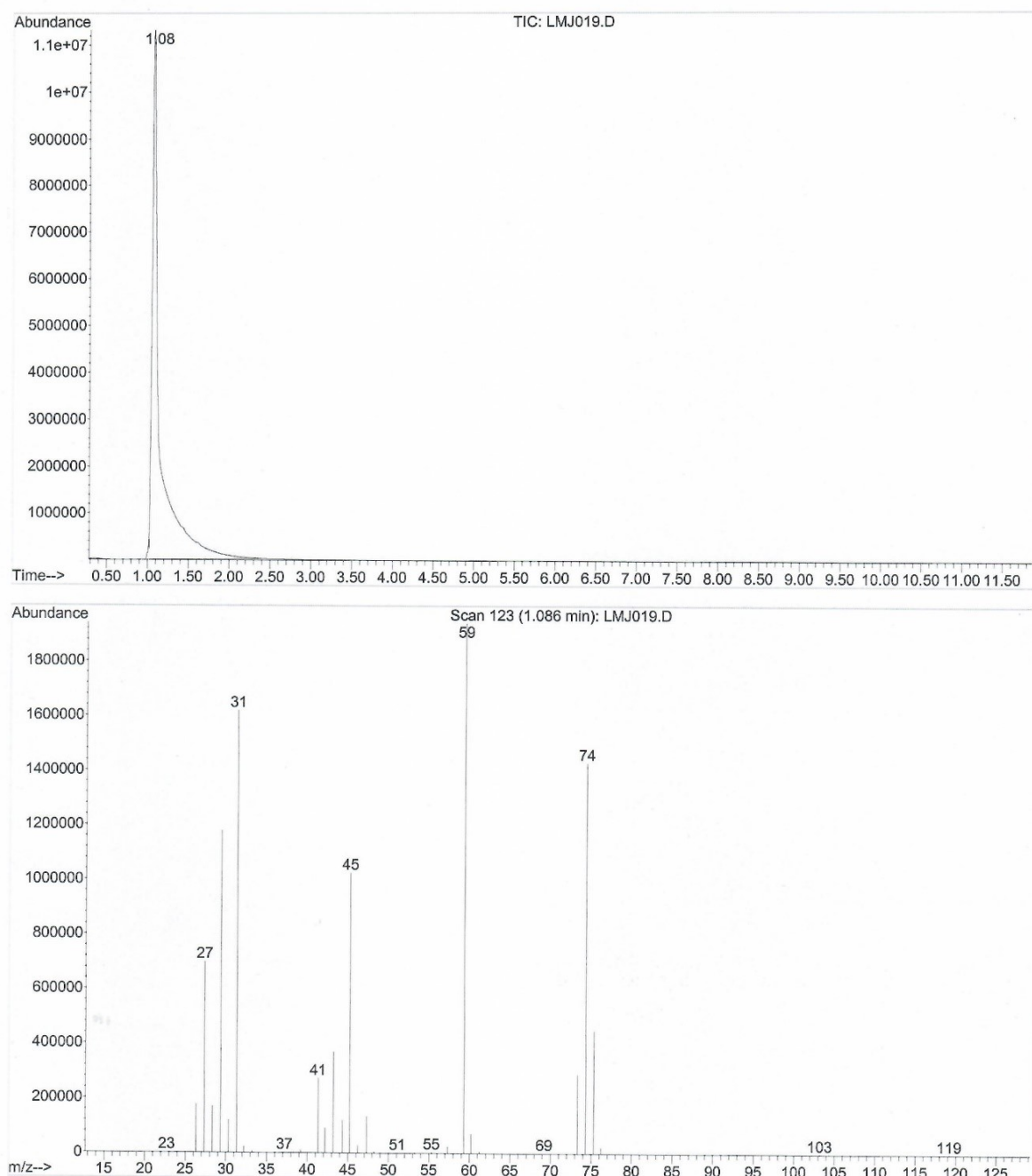
Method : C:\MSDCHEM\1\METHODS\DEFAULT.M (Chemstation Integrator)
 Title :

Signal : TIC

peak #	R.T. min	first scan	max scan	last scan	PK TY	peak height	corr. area	corr. % max.	% of total
1	1.073	93	121	196	BV 5	11331447	682183556	100.00%	88.322%
2	1.605	196	202	305	VB	2046168	90196487	13.22%	11.678%

Sum of corrected areas: 772380043

Fig. S22 GC-MS result of distilled diethyl ether containing Zn(NO₃)₂ for 1 day



Area Percent Report

Data File : C:\MSDCHEM\1\DATA\LMJ019.D Vial: 1
Acq On : 27 Dec 2021 13:24 Operator: LHK
Sample : LMJ D ether_Zn(NO₃)₂ Inst : Instrumen
Misc : 60/10/10/240 Multiplr: 1.00
Sample Amount: 0.00

MS Integration Params: autoint1.e

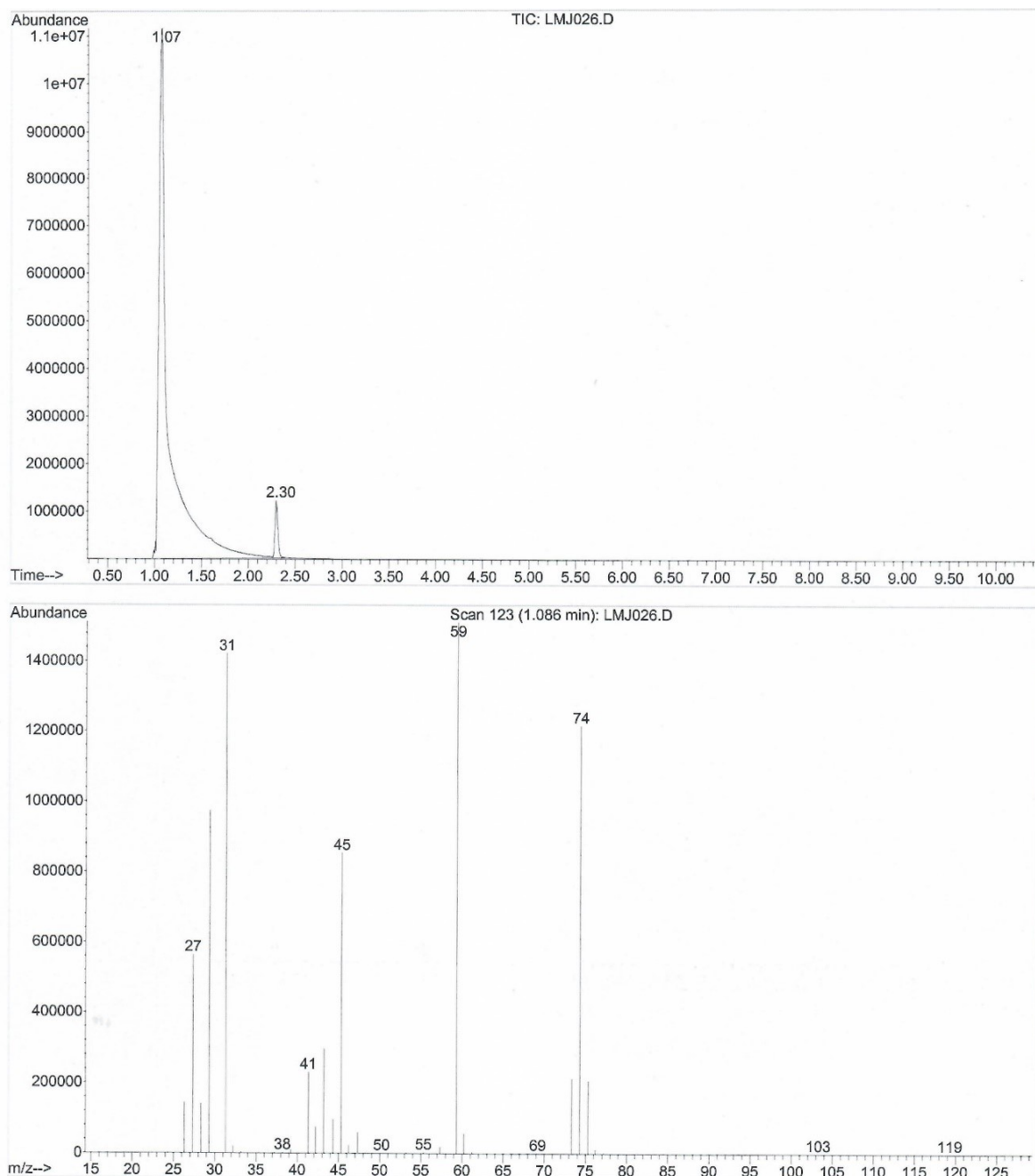
Method : C:\MSDCHEM\1\METHODS\DEFAULT.M (Chemstation Integrator)
Title :

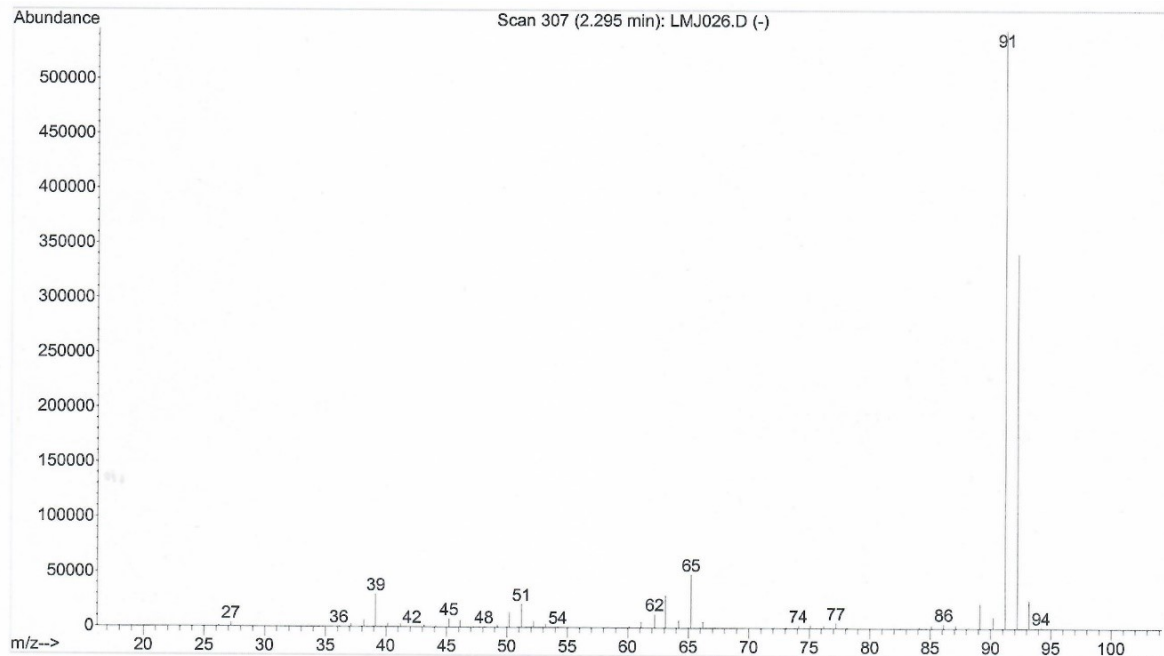
Signal : TIC

peak #	R.T. min	first scan	max scan	last scan	PK TY	peak height	corr. area	corr. % max.	% of total
1	1.080	97	122	329	BB	5	11328763	749202585	100.00% 100.000%

Sum of corrected areas: 749202585

Fig. S23 GC-MS result of distilled diethyl ether containing TBPG ligand for 1 day





Area Percent Report

Data File : C:\MSDCHEM\1\DATA\LMJ026.D Vial: 1
 Acq On : 28 Dec 2021 14:52 Operator: LHK
 Sample : LMJ D ether_ligand Inst : Instrumen
 Misc : 60/10710/240 Multiplr: 1.00
 Sample Amount: 0.00

MS Integration Params: autoint1.e

Method : C:\MSDCHEM\1\METHODS\DEFAULT.M (Chemstation Integrator)

Title :

Signal : TIC

peak #	R.T. min	first scan	max scan	last scan	PK TY	peak height	corr. area	corr. % max.	% of total
1	1.073	104	121	301	BV 4	11157777	797326498	100.00%	96.891%
2	2.302	301	308	329	VB	1181425	25585806	3.21%	3.109%

Sum of corrected areas: 822912304

Fig. S24 Fluorescence emission spectra of (*R*)-Zn and (*R,R*)-TBPG in the solid state

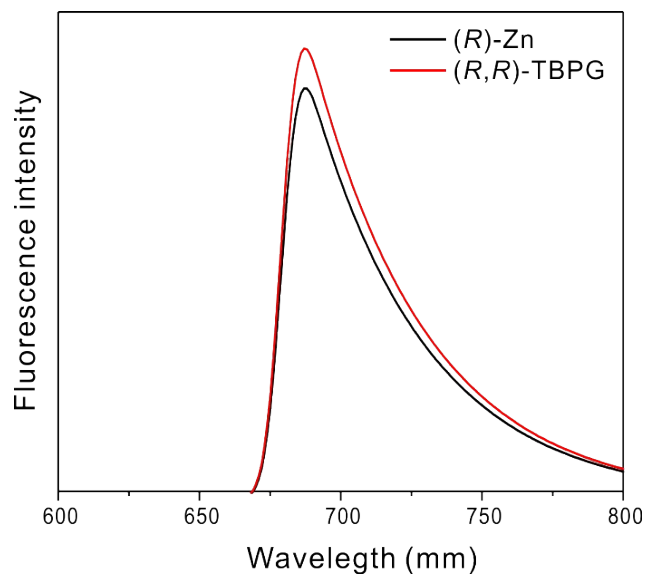


Fig. S25 PXRD patterns of (*R*)-Zn before and after the fluorescence measurements

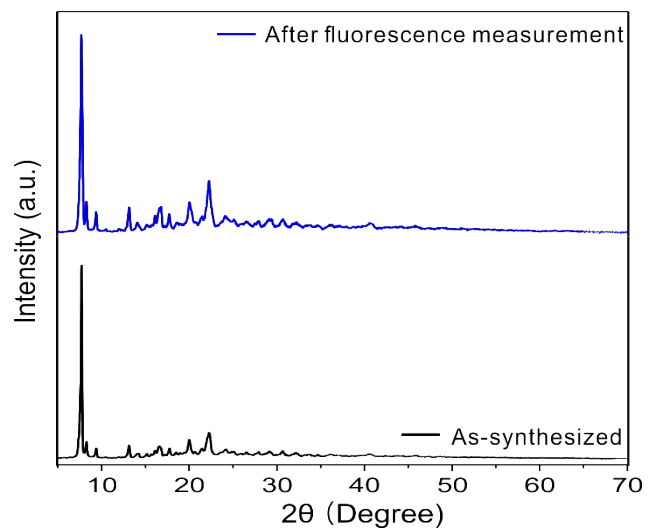


Fig. S26 Fluorescence emission spectra of (*R,R*)-TBPG upon addition of (a) D- and (b) L-histidine

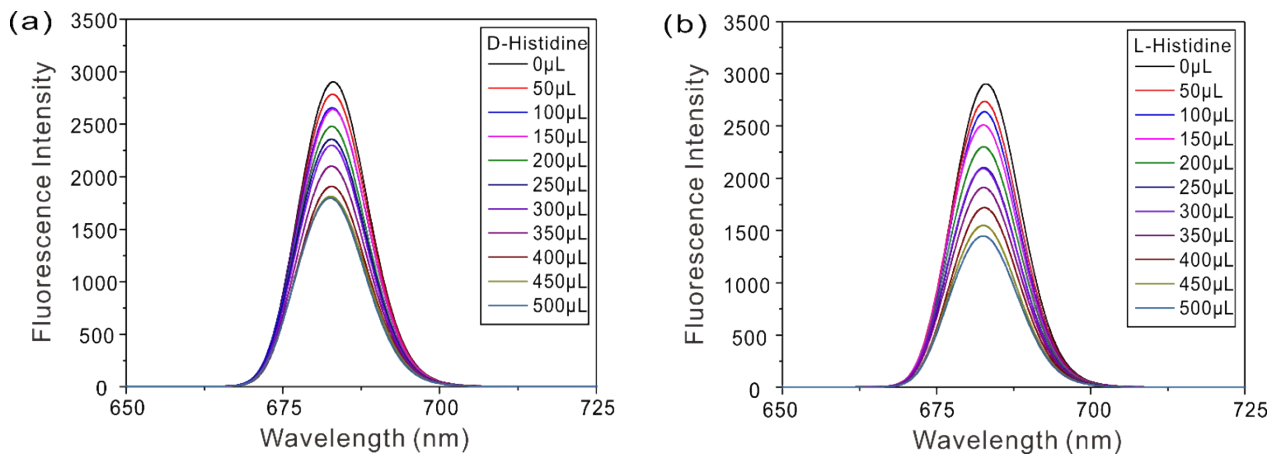


Fig. S27 Stern-Volmer (SV) plots of (*R,R*)-TBPG + D-histidine and (*R,R*)-TBPG + L-histidine

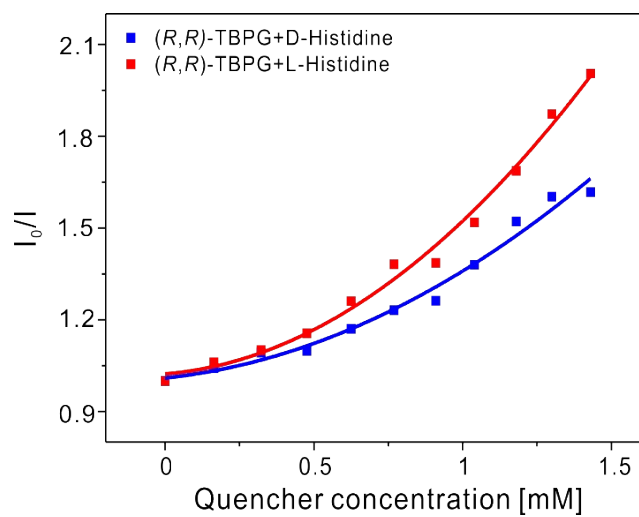


Fig. S28 Fluorescence emission spectra of (*R*)-Zn upon addition of imidazole

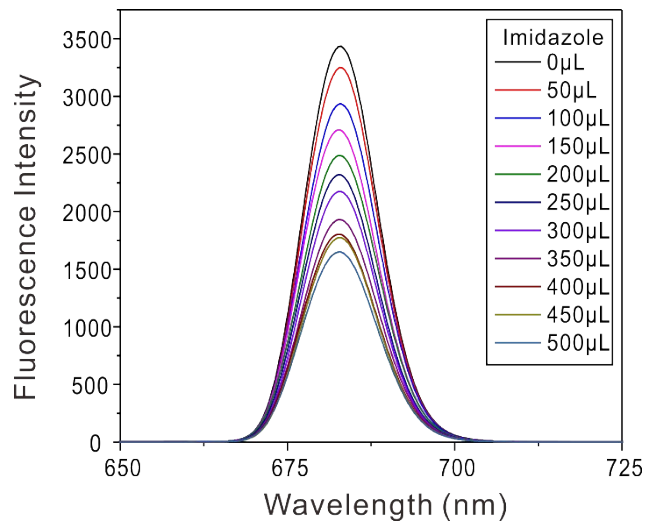


Fig. S29 Stern-Volmer (SV) plots of (*R*)-Zn + D-histidine, (*R*)-Zn + L-histidine and (*R*)-Zn + imidazole. The K_{SV} constant for (*R*)-Zn + imidazole is $7.6 \times 10^2 \text{ M}^{-1}$.

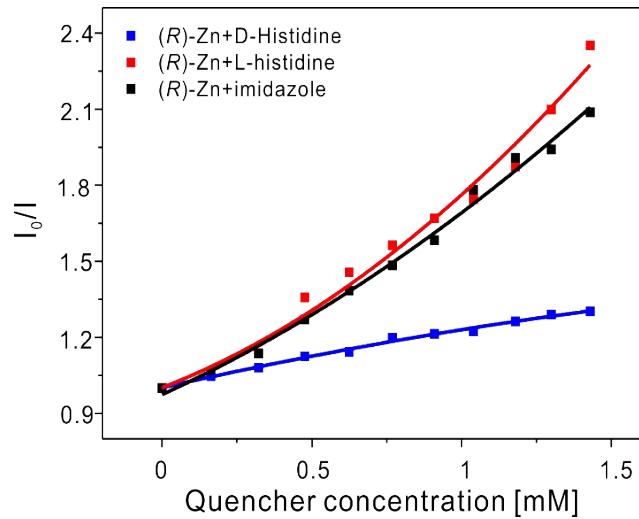


Fig. S30 ^1H NMR spectra for (R) -Zn in DMSO-d_6 , (R) -Zn + Histidine in $\text{DMSO-d}_6/\text{D}_2\text{O}$ and Histidine in D_2O

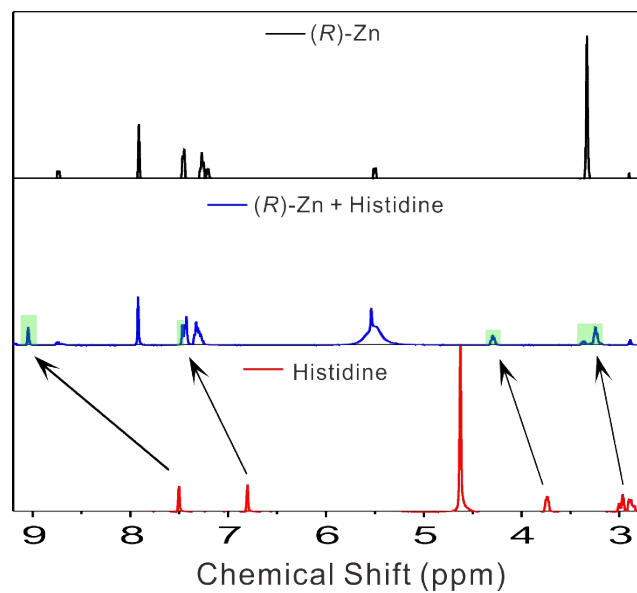


Fig. S31 Fluorescence emission spectra of (*S*)-Zn upon addition of (a) D- and (b) L-histidine

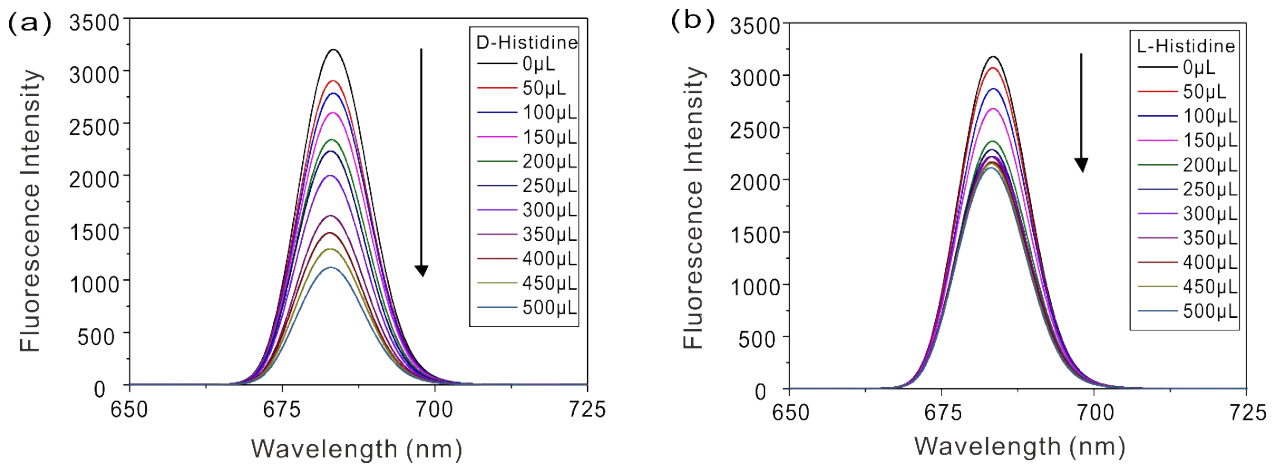
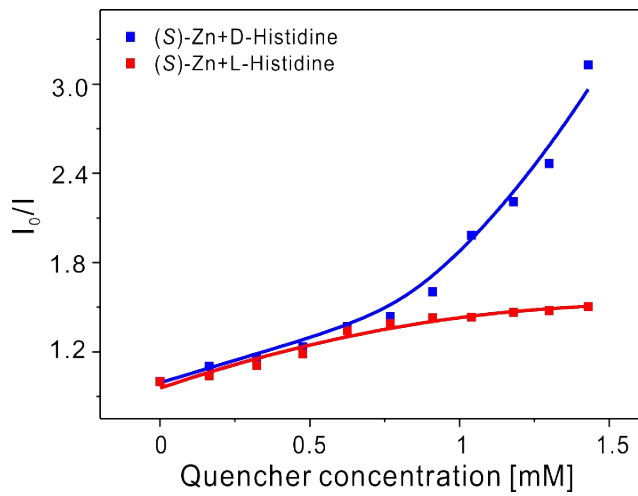


Fig. S32 Stern-Volmer (SV) plots of (*S*)-Zn + D-Histidine and (*S*)-Zn + L-Histidine. The K_{SV} constants for (*S*)-Zn + D-histidine and (*S*)-Zn + L-histidine are $1.5 \times 10^3 \text{ M}^{-1}$ and $3.5 \times 10^2 \text{ M}^{-1}$, respectively, and enantioselectivity factor α is calculated to be 4.22.



References

1. SADABS, Siemens Industrial Automation Inc, *Madison, WI*, 1996.
2. Siemens, Area-Detector Control and Integration Software, *Siemens Analytical X-ray Instruments Inc., Madison, WI, USA*, 1996.
3. R. H. Blessing, An empirical correction for absorption anisotropy, *Acta Crystallogr., A, Found. Crystallogr.*, 1995, **51**, 33-38.
4. G. Sheldrick, SHELXS-2013/1, program for the solution of crystal structures, *Germany: University of Göttingen*, 2013.
5. G. M. Sheldrick, Crystal structure refinement with SHELXL, *Acta Crystallogr. C Struct. Chem.*, 2015, **71**, 3-8.
6. L. J. Farrugia, WinGX and ORTEP for Windows: an update, *J. Appl. Crystallogr.*, 2012, **45**, 849-854.
7. A. L. Spek, PLATON SQUEEZE: a tool for the calculation of the disordered solvent contribution to the calculated structure factors, *Acta Crystallogr. C Struct. Chem.*, 2015, **71**, 9-18.
8. A. Spek, Single-crystal structure validation with the program PLATON, *J. Appl. Crystallogr.*, 2003, **36**, 7-13.
9. Z. Otwinowski and W. Minor, in *Methods Enzymol.*, Elsevier, 1997, vol. 276, pp. 307-326.
10. P. Kubelka, Ein Beitrag zur Optik der Farbanstriche (Contribution to the optic of paint), *Z. Tech. Phys.*, 1931, **12**, 593-601.
11. P. Giannozzi, S. Baroni, N. Bonini, M. Calandra, R. Car, C. Cavazzoni, D. Ceresoli, G. L. Chiarotti, M. Cococcioni and I. Dabo, QUANTUM ESPRESSO: a modular and open-source software project for quantum simulations of materials, *J. Phys.: Condens. Matter*, 2009, **21**, 395502.
12. D. Vanderbilt, Soft self-consistent pseudopotentials in a generalized eigenvalue formalism, *Phys. Rev. B*, 1990, **41**, 7892.
13. J. P. Perdew, K. Burke and M. Ernzerhof, Generalized gradient approximation made simple, *Phys. Rev. Lett.*, 1996, **77**, 3865.
14. S. Kurtz and T. Perry, A powder technique for the evaluation of nonlinear optical materials, *J. Appl. Phys.*, 1968, **39**, 3798-3813.
15. K. M. Ok, E. O. Chi and P. S. Halasyamani, Bulk characterization methods for non-centrosymmetric materials: second-harmonic generation, piezoelectricity, pyroelectricity, and ferroelectricity, *Chem. Soc. Rev.*, 2006, **35**, 710-717.